Sex-related differences in auditory processing in adolescents with fetal alcohol spectrum disorder: A magnetoencephalographic study

Claudia D. Tesche[a,*], Piyadasa W. Kodituwakku[a,b], Christopher M. Garcia[a], Jon M. Houck[a]

[a]Department of Psychology, University of New Mexico, Albuquerque, NM 87131, USA
[b]Department of Pediatrics, University of New Mexico Health Sciences Center, Albuquerque, NM 87131, USA

ABSTRACT

Children exposed to substantial amounts of alcohol in utero display a broad range of morphological and behavioral outcomes, which are collectively referred to as fetal alcohol spectrum disorders (FASDs). Common to all children on the spectrum are cognitive and behavioral problems that reflect central nervous system dysfunction. Little is known, however, about the potential effects of variables such as sex on alcohol-induced brain damage. The goal of the current research was to utilize magnetoencephalography (MEG) to examine the effect of sex on brain dynamics in adolescents and young adults with FASD during the performance of an auditory oddball task. The stimuli were short trains of 1 kHz "standard" tone bursts (80%) randomly interleaved with 1.5 kHz "target" tone bursts (10%) and "novel" digital sounds (10%). Participants made motor responses to the target tones. Results are reported for 44 individuals (18 males and 26 females) ages 12 through 22 years. Nine males and 13 females had a diagnosis of FASD and the remainder were typically-developing age- and sex-matched controls. The main finding was widespread sex-specific differential activation of the frontal, medial and temporal cortex in adolescents with FASD compared to typically developing controls. Significant differences in evoked-response and time–frequency measures of brain dynamics were observed for all stimulus types in the auditory cortex, inferior frontal sulcus and hippocampus. These results underscore the importance of considering the influence of sex when analyzing neurophysiological data in children with FASD.

1. Introduction

Exposure to moderate to heavy amounts of alcohol during pregnancy remains a leading preventable cause of intellectual disabilities in North America (Abel and Sokol, 1986; May and Gossage, 2001; Chudley et al., 2005; May et al., 2009). Children with fetal alcohol spectrum disorder (FASD) face a broad spectrum of cognitive and behavioral challenges, including deficits in sensory processing, attention, working memory and executive function (Mattson et al., 1998; Roussotte et al., 2010; Mattson et al., 2011; Riley et al., 2011). Although facial dysmorphia is characteristic of fetal alcohol syndrome (FAS), the severe end of the FASD spectrum, many children with FASD lack physical abnormalities and hence are often not diagnosed, even though sharing many of the same cognitive and behavioral issues (Mattson et al., 1998; Kodituwakku, 2009; Roussotte et al., 2010; Mattson et al., 2011). This latter group of children, labeled as showing alcohol related neurodevelopmental disorder (ARND), is known to display aberrant neural functions and subtle neuroanatomical differences in neuroimaging studies.

Delayed and/or abnormal brain development may contribute to deficits in cognitive function and increased behavioral issues in adolescents with FASD (Lebel et al., 2011; Triet et al., 2013). Brain regions particularly vulnerable to alcohol's teratogenicity include the frontal and parietal cortex, posterior sensory cortex, caudate, hippocampus, and cerebellum (for a review, see Roussotte et al., 2010). Although reduction in total brain volume is a common feature in FASD (Astley et al., 2009; Lebel et al., 2011), increased local cortical thickness has been reported in the parietal and frontal cortices (Sowell et al., 2002; Sowell et al., 2008) and in the inferior frontal, superior temporal, and middle temporal cortex (Yang et al., 2012). Yang et al., 2012 found that even children with ARND showed volume reductions in multiple brain regions, including the frontal, parietal, and temporal lobes,

although these volume reductions were due to reduced cortical surface area rather than thickness. Abnormal and delayed development of white matter tracts have also been seen in FASD in the posterior corpus callosum, anterior–posterior fiber bundles, superior longitudinal fasciculus and superior and inferior fronto-occipital fasciculus, and cerebellar peduncles (cf. Wozniak et al., 2011a,b; Spottiswoode et al., 2011; Triet et al., 2013; Green et al., 2013).

Adolescence is a period of marked change in brain organization. Functional neuroimaging studies reveal that typically developing adolescents exhibit weaker modulatory control from frontal areas compared to adults (Hwang et al., 2010). In a recent fMRI study of children from 7–14 years of age, FASD showed reduced activation bilaterally in the frontal, parietal and temporal cortex compared to controls, suggesting an impact of alcohol exposure *in utero* on maturation (Gautam et al., 2014). Increased frontal and parietal activation has been reported during the performance of spatial working memory task in ARND and go/no-go tasks in FASD (Malisza et al., 2012; Norman et al., 2013; O'Brien et al., 2013). Although differences observed in microvascular networks in a mouse model of FAS/partialFAS suggest some caution in the interpretation of these fMRI data (Jégou et al., 2012), electroencephalographic (EEG) and magnetoencephalographic (MEG) studies also support differences in measures of brain function in FASD. Deficits in auditory stimulus classification and inhibition have been reported in adolescents with FAS/partialFAS (Steinmann et al., 2011). Latency and amplitude differences of the P300 auditory event-related potential (ERP) in an oddball task discriminated between children with Down syndrome, FASD, and typically developing controls (Kaneko et al., 1996a). Auditory processing delays have also been observed in a MEG study of preschool children with FASD (Stephen et al., 2012).

The present study utilized MEG to investigate brain dynamics of adolescents with FASD during the performance of an auditory oddball task. This task probes development of a "top-down" perceptual expectation for a set of repeated (standard) tones, detection of "target" tones that elicit behavioral responses and processing of novel digital sounds in cortico-hippocampal circuits (Halgren et al., 1998). Sex-related differences in brain structure are known to emerge in typically developing adolescents, with increased volume of the amygdala in males and of the hippocampus in females (for a review, see Blakemore, 2012). Since prenatal ethanol exposure is known to produce sex-specific deficits in hippocampus in rodent models (Coleman et al., 2012; see also Helfer et al., 2012; Sickmann et al., 2014), we hypothesized that MEG measures of brain activation in the oddball data may reveal sex-specific differences for adolescents with FASD. Consideration of potential sexual dimorphism in neuroimaging and neurophysiological studies in adolescents with FASD is rare (although see Kaneko et al., 1996a).

The present effort will contribute novel information on sex-specific effects on brain function and motivate further attention to potential sexual dimorphism in studies of adolescents with FASD.

2. Methods

2.1. Participants

Forty eight adolescents and young adults in the age range 12–22 years were recruited for this study. High quality MEG data were obtained from 44 participants. One of these participants did not complete the MRI scan. For the participants utilized in the MEG analysis, twenty two of the participants (9 male, age 15.0 yrs, SD = 3.6 yrs; 13 female, age 15.5 yrs, SD = 2.8 yrs) were identified as FASD according to the modified Institute of Medicine criteria (Stratton et al., 1996). Of these, 9 were diagnosed with FAS (6 male and 3 female) and 13 with alcohol-related neurodevelopmental disorder (ARND) (3 male and 10 female). Twenty-two age- and sex-matched healthy individuals (HC; 9 male, M age 13.5 yrs, SD = 4.7 yrs; 13 female, M age 16.8 yrs, SD = 3.3 yrs) with no history of

prenatal alcohol exposure, developmental delays, significant psychiatric or neurological problems served as controls. All of the participants were right handed (Edinburgh Handedness Inventory: Oldfield, 1971) and none of the participants had significant sensory problems (*e.g.* poor vision or hearing) or difficulty understanding the task demands.

Participants with FASD were recruited at the University of New Mexico Fetal Alcohol Diagnostic and Evaluation Clinic and healthy controls (HC) through flyers and word of mouth.

This study was approved by the University of New Mexico Health Sciences Center Institutional Review Board and was in full compliance with The Code of Ethics of the World Medical Association (Declaration of Helsinki). Informed consent was obtained from the parents/legal guardians and/or participants dependent on the age and assent from minors in accord with the Institutional Review Board guideline of the University of New Mexico. Participants were compensated for their time and travel expenses.

Table 1
Comparison of FASD and HC on neuropsychological measures, response times to target stimuli and age.

Group comparisons:						
Measure	FASD		HC		d	t (df)
	Mean	SD	Mean	SD		
IQ	81.78	10.05	100.47	9.93	1.87	5.53* (33)
Vocab	31.00	7.36	49.53	8.62	2.31	6.86* (33)
Matrix Reas	44.89	9.24	49.76	8.76	0.54	1.60 (33)
RT (ms)	579.58	157.99	514.86	94.06	−0.50	−1.54 (37)
Age (years)	17.30	2.66	17.37	2.61	0.03	0.08 (37)

Between group sex comparisons:						
Measure	FASDM		HCM		d	t (df)
	Mean	SD	Mean	SD		
IQ	78.88	12.46	101.11	8.1	2.28	4.42* (15)
Vocab	29.50	7.09	50.0	7.05	3.08	5.97* (15)
Matrix Reas	41.88	11.34	48.78	10.85	0.66	1.28 (15)
RT (ms)	575.52	133.47	480.31	110.78	−0.82	−1.59 (15)
Age (years)	16.0	2.92	16.3	2.72	0.11	0.24 (18)
Measure	FASDF		HCF		d	t (df)
	Mean	SD	Mean	SD		
IQ	82.25	8.07	99.08	11.0	1.82	4.27* (22)
Vocab	31.55	7.63	48.42	9.95	1.98	4.53* (21)
Matrix Reas	46.45	7.06	50.58	5.4	0.69	1.58 (21)
RT (ms)	611.61	204.45	507.19	83.50	−0.69	−1.65 (23)
Age (years)	15.91	3.16	16.55	3.14	0.21	0.53 (25)

Within group sex comparisons:						
Measure	HCM		HCF		d	t (df)
	Mean	SD	Mean	SD		
IQ	101.11	8.1	99.08	11.0	−0.213	−0.465 (19)
Vocab	50.0	7.05	48.42	9.95	−0.186	−0.406 (19)
Matrix Reas	48.78	10.85	50.58	5.4	0.230	0.502 (19)
RT (ms)	480.31	110.78	507.19	83.50	0.292	0.620 (18)
Age (years)	16.3	2.72	16.55	3.14	0.089	0.209 (22)
Measure	FASDM		FASDF		d	t (df)
	Mean	SD	Mean	SD		
IQ	78.88	12.46	82.25	8.07	−0.348	0.739 (18)
Vocab	29.50	7.09	31.55	7.63	0.288	0.594 (17)
Matrix Reas	41.88	11.34	46.45	7.06	0.527	1.086 (17)
RT (ms)	575.52	133.47	611.61	204.45	0.208	0.464 (20)
Age (years)	16.0	2.92	15.91	3.16	−0.028	−0.065 (21)

Note. FASD = fetal alcohol spectrum disorder. HC = healthy control. d = Cohen's d. RT = response time. IQ = full scale IQ from WASI. All effects computed as HC-FASD or male (M)–female (F).
* p ≤ .05.

2.2. Cognitive assessment

Cognitive assessment was performed at the MIND Research Network in conjunction with the MEG/MRI scans. Two subtests from the Wechsler Abbreviated Scale of Intelligence (WASI, Vocabulary and Matrix Reasoning) were utilized to compute full scale IQ.

2.3. Auditory stimuli

Stimuli for the auditory oddball task were 1 kHz "standard" tone bursts (80%), 1.5 kHz "target" tone bursts (10%) and "novel" digital sounds (10%) presented binaurally through plastic tubes placed into the ear canals. The standard tones occurred sequentially in sets of 3–5 stimuli. Target and novel stimuli were randomly interleaved between

Table 2
Latency and onset of auditory evoked-response to standard stimuli.

Hemisphere and component	FASD		HC		d	t (df)
	Mean	SD	Mean	SD		
L P50m	49.12	8.70	52.29	7.28	0.40	1.24 (38)
L N100m onset	64.22	10.57	71.74	9.91	0.76	2.27* (36)
L N100m	90.24	14.02	100.0	12.27	0.79	2.37* (39)
R P50m	46.12	9.57	46.22	10.40	0.01	0.034 (36)
N100m onset	63.47	9.63	65.56	11.50	0.19	0.503 (27)
N100m	90.79	8.99	90.47	10.96	0.03	0.100 (38)
Hemisphere and component	FASDF		FASDM		d	t (df)
	Mean	SD	Mean	SD		
L P50m	46.4	8.98	53.55	6.46	0.89	1.95 (19)
L N100m onset	60.41	9.95	70.71	8.70	1.11	2.28* (17)
L N100m	86.55	14.14	96.24	12.34	0.73	1.60 (19)
R P50m	39.8	7.05	54.8	3.93	2.62	5.41* (17)
R N100m onset	57.77	6.32	70.32	8.62	1.86	2.79* (9)
R N100m	89.73	11.11	92.61	3.18	0.32	0.67 (17)
Hemisphere and component	HCF		HCM		d	t (df)
	Mean	SD	Mean	SD		
L P50m	50.17	5.85	55.21	8.40	0.75	1.55 (17)
L N100m onset	65.92	8.47	79.75	4.81	2.01	4.14* (17)
L N100m	93.75	8.56	109.38	11.21	1.67	3.54* (18)
R P50m	41.82	8.86	52.29	9.68	1.19	2.45* (17)
R N100m onset	61.66	11.23	71.69	9.63	0.98	1.95 (16)
R N100m	85.90	10.09	97.90	8.16	1.3	2.83* (19)
Hemisphere and component	FASDF		HCF		d	t (df)
	Mean	SD	Mean	SD		
L P50m	46.4	8.98	50.17	5.85	0.51	1.19 (22)
L N100m onset	60.41	9.95	65.92	8.47	0.62	1.42 (21)
L N100m	86.55	14.14	93.75	8.56	0.64	1.53 (23)
R P50m	39.8	7.05	41.82	8.86	0.26	0.59 (20)
R N100m onset	57.77	6.32	61.66	11.23	0.40	0.78 (15)
R N100m	89.73	11.11	85.90	10.09	0.40	0.90 (23)
Hemisphere and component	FASDM		HCM		d	t (df)
	Mean	SD	Mean	SD		
L P50m	53.55	6.46	55.21	8.40	0.24	0.44 (14)
L N100m onset	70.71	8.70	79.75	4.81	1.41	2.54* (13)
L N100m	96.24	12.34	109.38	11.21	1.19	2.23* (14)
R P50m	54.8	3.93	52.29	9.68	0.36	0.68 (14)
R N100m onset	70.32	8.62	71.69	9.63	0.16	0.25 (10)
R N100m	92.61	3.18	97.90	8.16	0.89	1.60 (13)
Hemisphere and component	HC left		HC right		d	t (df)
	Mean	SD	Mean	SD		
P50m	52.07	7.64	47.06	10.61	0.47	1.95 (16)
N100m onset	72.38	10.36	66.26	12.03	0.55	2.20* (15)
N100m	100.0	12.27	91.33	10.49	0.71	3.16* (19)
Hemisphere and component	FASD left		FASD right		d	t (df)
	Mean	SD	Mean	SD		
P50m	48.33	8.50	46.12	9.57	0.20	0.85 (18)
N100m onset	64.09	4.55	62.21	6.57	0.25	0.75 (8)
N100m	94.72	10.56	90.46	9.14	0.27	1.14 (17)

Note. FASD = fetal alcohol spectrum disorder. HC = healthy control. d = Cohen's d. All effects computed as HC-FASD or male (M)–female (F).
* $p \leq 05$.
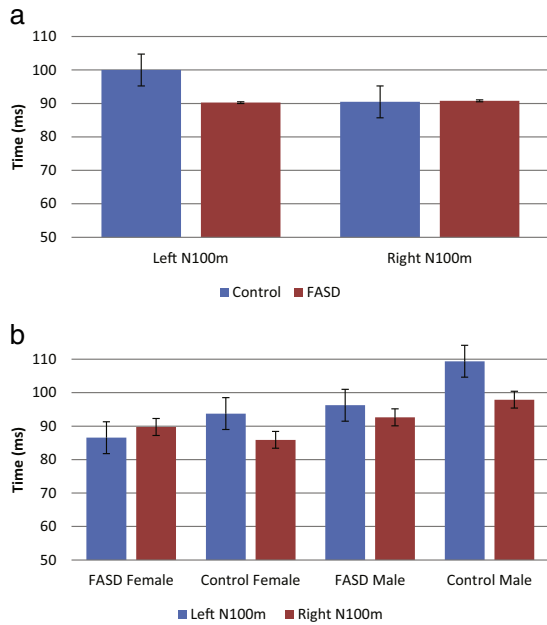
Fig. 1. Left and right hemisphere N100m auditory evoked-response latencies determined in and near the posterior ramus of the lateral sulcus following standard tones. a) Results for 22 adolescents and emerging adults with FASD and 22 age- and sex-matched controls. b) Results for 9 males with FASD, 9 male controls, 13 females with FASD and 13 female controls.

the sets of standard stimuli. The duration of all stimuli was 200 ms with a pseudorandom stimulus onset asynchrony between the stimuli of 1–3 s (mean 1.5 s) and intensity of 85 dB. The stimuli were grouped into four equal-duration blocks, with brief rest intervals (1–5 min) between blocks. The total number of stimuli in all four blocks was 784 (standard), 98 (target) and 98 (novel). Participants were asked to press a response button with the right index finger upon perception of the 1.5 kHz target tones. A short training period was conducted before the commencement of the MEG scan. Presentation software (http://www.neurobs.com) was used to deliver stimuli and record motor responses to target stimuli.

2.4. Data acquisition

Magnetoencephalographic (MEG) data were acquired at the Mind Research Network (MRN, Albuquerque, NM). Participants were seated inside a double-layer magnetically shielded room (Vacuumschmelze) under a 306-channel MEG array (Elekta Neuromag™) and monitored throughout the scan. A parent or guardian was present in the room when requested. Prior to the scan, a Polhemus 3D position tracker was used to record the location of four head positioning (HPI) coils on the left and right mastoid and bilaterally on the forehead and the left and right preauricular and nasion fiducial points. Multiple scalp and face locations were also recorded.

The MEG data were sampled at 1200 Hz and band-pass filtered on-line at 0.1–330 Hz. The location of the participant's head with respect
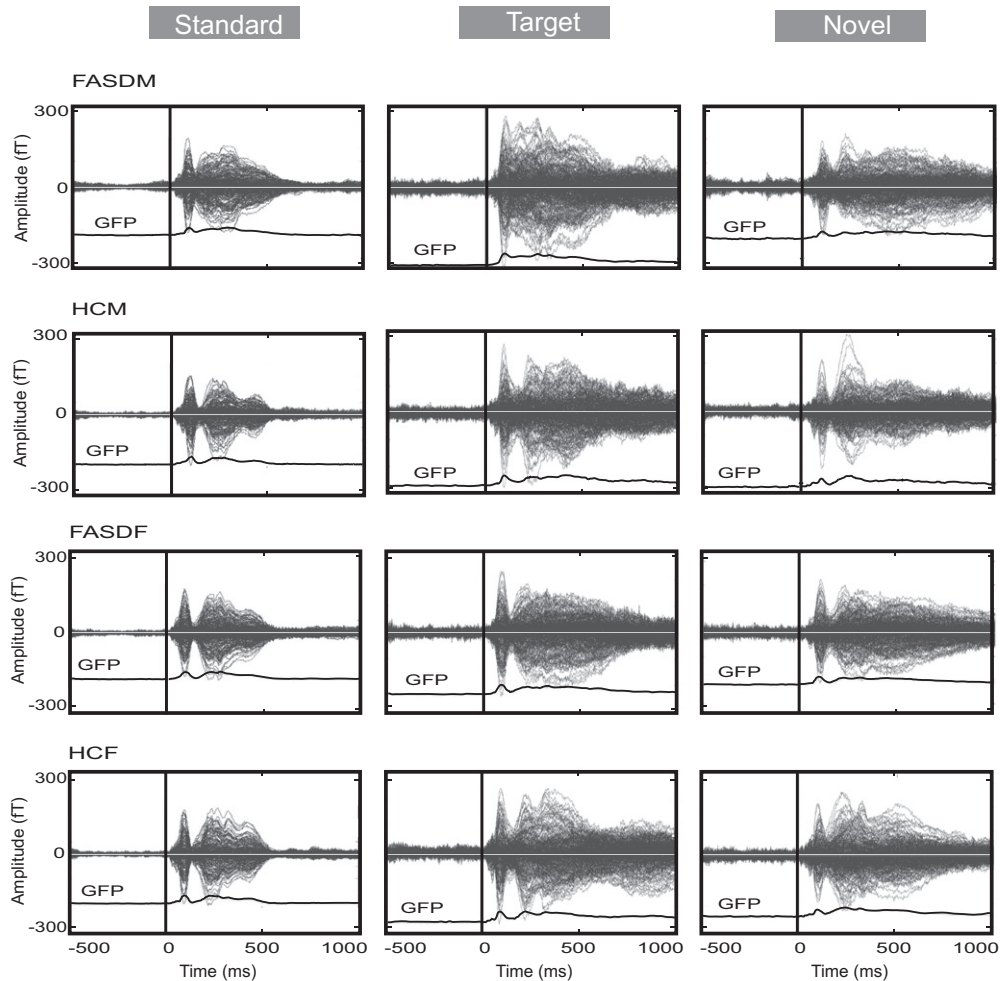

Fig. 2. MEG sensor amplitudes and global field power (GFP) in femtotesla (fT) as a function of time for standard, target and novel trials. The auditory stimuli were presented at t = 0 ms. Data were averaged across all participants for 9 males with FASD (FASDM), 9 age- and sex-matched controls (HCM), 13 females with FASD (FASDF) and 13 age- and sex-matched controls (HCF).
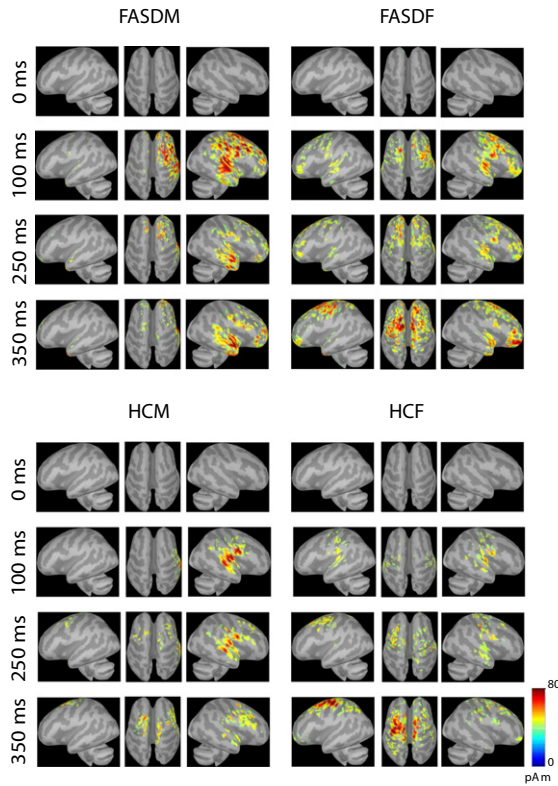
Fig. 3. Group-averaged brain activation patterns for male (FASDM) and female (FASDF) participants with FASD and male (HCM) and female (HCF) healthy controls. Data are shown for the absolute value of dipolar current flow in picoAmp meter (pAm) at 0, 100, 250 and 350 ms following presentation of standard stimuli at t = 0 ms.
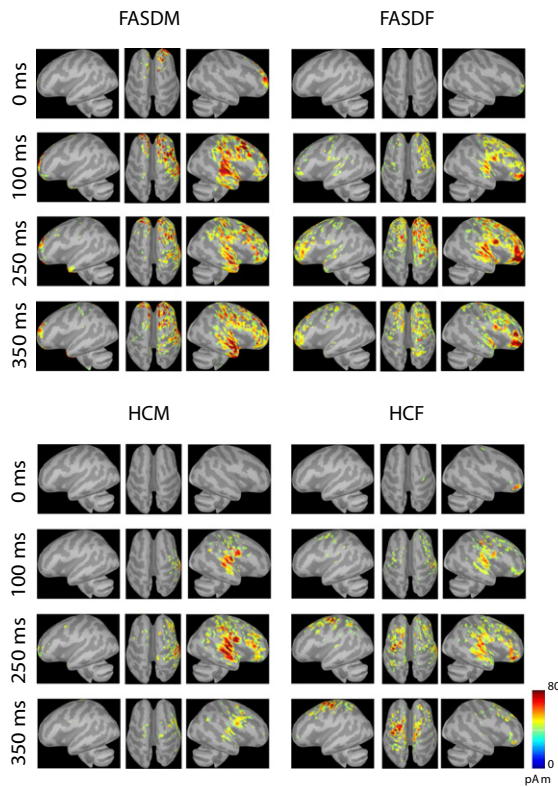
Fig. 4. Group-averaged brain activation patterns for male (FASDM) and female (FASDF) participants with FASD and male (HCM) and female (HCF) healthy controls. Data are shown for the absolute value of dipolar current flow in picoAmp meter (pAm) at 0, 100, 250 and 350 ms following presentation of target stimuli at t = 0 ms.
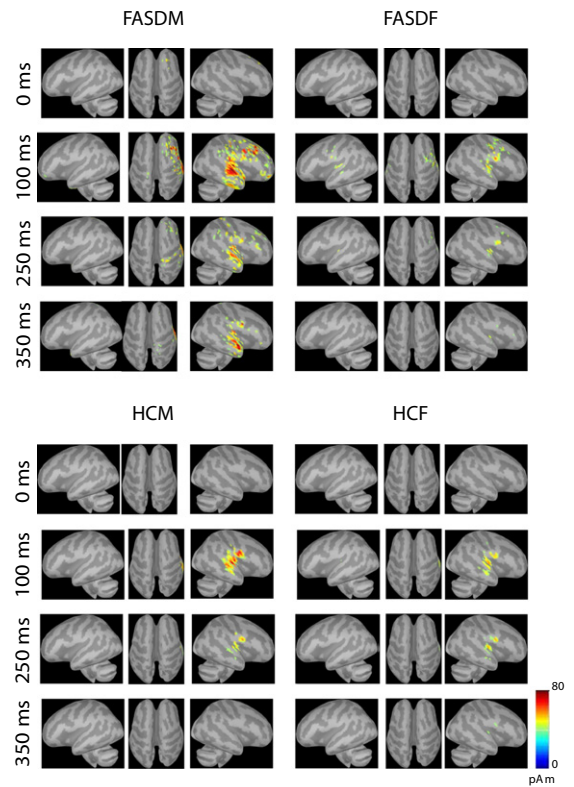
Fig. 5. Group-averaged brain activation patterns for male (FASDM) and female (FASDF) participants with FASD and male (HCM) and female (HCF) healthy controls. Data are shown for the absolute value of dipolar current flow in picoAmp meter (pAm) at 0, 100, 250 and 350 ms following presentation of novel stimuli at t = 0 ms.

to the MEG array was recorded throughout the scan through activation of the HPI coils. Bipolar horizontal and vertical electro-oculograms and a bipolar electrocardiogram were recorded throughout the scan. All data were recorded for off-line analysis.

High-resolution T_1-weighted anatomic images were acquired using a 3T Siemens Trio TIM with a multi-echo magnetization prepared rapid gradient echo (MPRAGE) sequence (echo time [TE] = 1.64, 3.5, 5.36, 7.22, and 9.08 ms; repetition time [TR] = 2530 ms; inversion time [TI] = 1200 ms; flip angle = 7°; number of excitations = 1; slice thickness = 1 mm; field of view [FOV] = 256 mm; resolution = 256×256 mm). The scan session lasted approximately 30 min and also included functional MRI (fMRI) and diffusion tensor imaging (DTI) acquisition, which are not included in this manuscript. The average image (root-mean-square) across the five echoes of the MPRAGE was used for co-registration with MEG data and for construction of a boundary element model (BEM) for each participant.

2.5. MEG and MRI data analysis

Elekta Neuromag Maxfilter™ software was used to compensate for head movement under the scanner and to remove artifacts originating outside the cranial volume (Taulu and Simola, 2006). All data for each subject were co-located to a common subject-specific head position. Signal-space projectors were created from these data and used to further suppress blink and cardiac signals on an individual subject basis (Tesche et al., 1995; Tesche et al., 1995). The data were down-sampled at 600 Hz and averaged time-locked to stimulus presentation for each stimulus type (standard, target, novel) for epochs of 500 ms before to 1000 ms after auditory stimulus presentations. The evoked-response averages were baseline corrected from 500 to 0 ms before stimulus presentation. Since activity at 1000 ms after stimulation occurred immediately before the earliest possible presentation of a

subsequent stimulus (the minimum ISI between all stimuli was 1000 ms), the evoked-response waveforms were terminated at 1000 ms to avoid contamination with the processing induced by subsequent stimuli.

Surface tessellation of the cerebral and of the cerebellar cortex was extracted from each participant's MR images using BrainSuite (http://brainsuite.org). Each surface was approximated by a grid of 7000 points. The cerebral and cerebellar cortical tessellations were merged to form a brain-based source space for MEG data inversion. A similar cortico-cerebellar tessellation was constructed from MR images for the Collin 27 adult brain (Collins, 1998) which was used as a common source space for all between-subject analyses.

Brainstorm (Tadel et al., 2011) was used to compute average sensor waveforms and global field power plots from the MEG sensor data and to extract brain-based waveforms for specific brain regions. Brainstorm is a documented and freely available package downloaded online under a GNU general public license (http://neuroimage.usc.edu/brainstorm/). The MEG data were co-localized with the structural MRI data on an individual participant basis. Source-space waveforms were then computed for each participant from all sensor evoked-response data (utilizing both gradiometer and magnetometer sensor data) and the individual brain surface tessellation using a weighted minimum norm estimate (wMNE).

The P50m and N100m responses were determined for each participant from their individual MEG/MRI data. An initial region of interest was selected in and near the posterior ramus of the lateral sulcus. A waveform of activation for this ROI was then extracted from the participant's evoked-response data and the latency of the peak response noted. The initial ROI was adjusted on an iterative basis to encompass the region of activation at the peak latency. This procedure was followed for activation between 40 and 70 ms for the P50m response and independently at 80–120 ms for the N100m response. This analysis was performed blinded to the sex or diagnosis of the participant. When these cortical areas corresponding to the P50m and N100m responses were projected onto the Colin 27 brain, variable blurring and shifting of the ROIs across participants were observed. More representative individual latency values used in the present study were determined using each participant's MRI before the transformation of the source data into the Colin 27 brain.

Group-averaged brain activation patterns were determined by projection of each participant's source-space data onto a common surface derived from the Collin 27 brain. Averages of the absolute value of individual activation patterns within this source space were determined for the standard, target and novel trials separately for male and female FASD and the sex- and age-matched controls. One participant did not have an MRI. MEG data for this subject were projected directly onto the Colin 27 brain using a Polhemus digitization of the participant's face and scalp. Brain activation patterns were determined for all participants at 100, 250 and 350 ms after stimulus presentation.

Waveforms of brain activity were computed within Brainstorm from group averages of the absolute value of source activation data. The following regions were selected as salient for stimulus processing and novelty detection: the posterior ramus of the lateral sulcus and the inferior frontal sulcus as described in the Destrieux cortical atlas (Destrieux
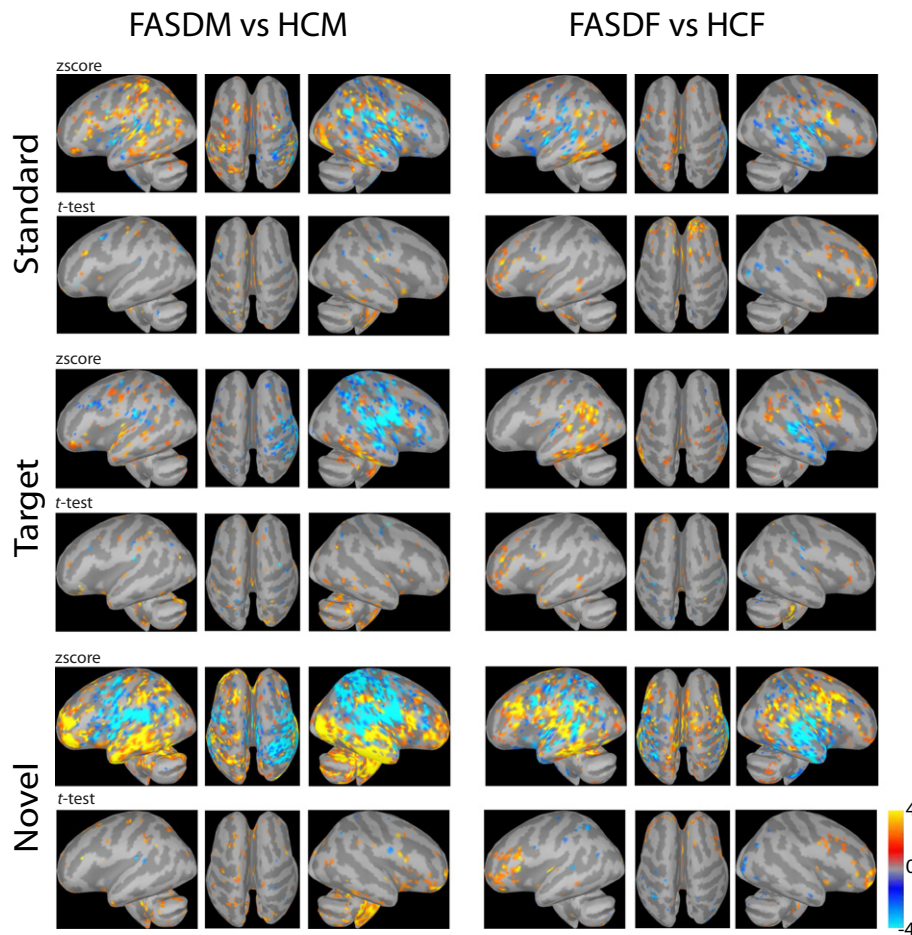
Fig. 6. Comparison of group-averaged brain activation patterns for FASD vs. age- and sex-matched healthy controls at 100 ms following presentation of the standard, target and novel stimuli. The z-score plots show the difference of the mean brain activation for FASDM vs. HCM and for FASDF vs. HCF. The absolute values of the current flow at each location were normalized for each individual participant to the baseline activation from 500 to 0 ms before stimulus presentation. The corresponding t-test plots were thresholded at p < 0.05.

et al., 2010) and the hippocampus as determined from the Collin 27 images within Brainstorm.

2.6. Statistical analysis

Comparisons of FASD and HC were calculated for neuropsychological measures, response times to target stimuli and age (Table 1). All statistical analysis was completed using IBM SPSS Statistics 19. Levene's Test for equality of variances were performed for all comparisons. If significant, the corrected t or F statistic was used. All statistics were calculated two-tailed and the critical value for rejecting the null hypothesis was $p \le 0.05$. To assess performance on the Oddball task, response times (RTs) and accuracy to the target stimuli were extracted from logfiles generated by presentation and averaged for each block. A grand average was computed for each participant across all trials. The raw scores for the Vocabulary and Matrix Reasoning subtests from the WASI were T scored and used to determine the participant's IQ score. FASD and control group performance on the Oddball task, and WASI were then compared using independent samples t-tests. Performance was further explored by comparing sex differences by group and then within group. To test for a difference in age an independent samples t-test was performed. To test for difference in sex, a Chi-squared test was performed.

Independent samples t-tests were performed to evaluate the differences between FASD and HC groups for latency measures of the auditory evoked-response to standard stimuli (P50m, N100m, and N100m

onsets) (Table 2). Differences in latencies were further explored by comparing sex differences by group and then within group. A 2 × 3 Repeated Measures ANOVA was performed to compare the left hemisphere P50m, N100m, and N100m latencies by group. A separate 2 × 3 Repeated Measures ANOVA was performed to compare the right hemisphere P50m, N100m, and N100m latencies by group. Within subject lateralization differences were tested using paired-sample t-tests.

Pearson's correlations were executed to examine relationships between the auditory evoked-response latencies and the behavioral, neuropsychological and age data. These relationships were further explored by comparing sex differences both between groups and within group.

Brainstorm (Tadel et al., 2011) was used to compute brain activation patterns for FASDM, FASDF, HCM and HCF (Figs. 3–5). The data were averaged for standard, target and novel trials at 0, 100, 250 and 350 ms following stimulus presentation. In Brainstorm, the visualization parameter amplitude was set to 50% and the minimum size was set to 1 (all features of every size are displayed). Comparison of activation plots for FASDM vs. HCM and for FASDF vs. HCF was also computed in Brainstorm (Figs. 6–8). The activation plots for each participant were normalized to baseline values from −500 to 0 ms prior to computation of group-averaged data. Mean difference and t-test plots were then computed from the normalized data. The p-value threshold for the t-test plots was 0.05. The comparisons between groups of evoked-response waveforms were performed using a matched-pair (sex and age) t-test on each sampled instant (Figs. 9, 11, 13). Epochs of significant differences ($p < 0.01$) were computed from the data and are indicated as
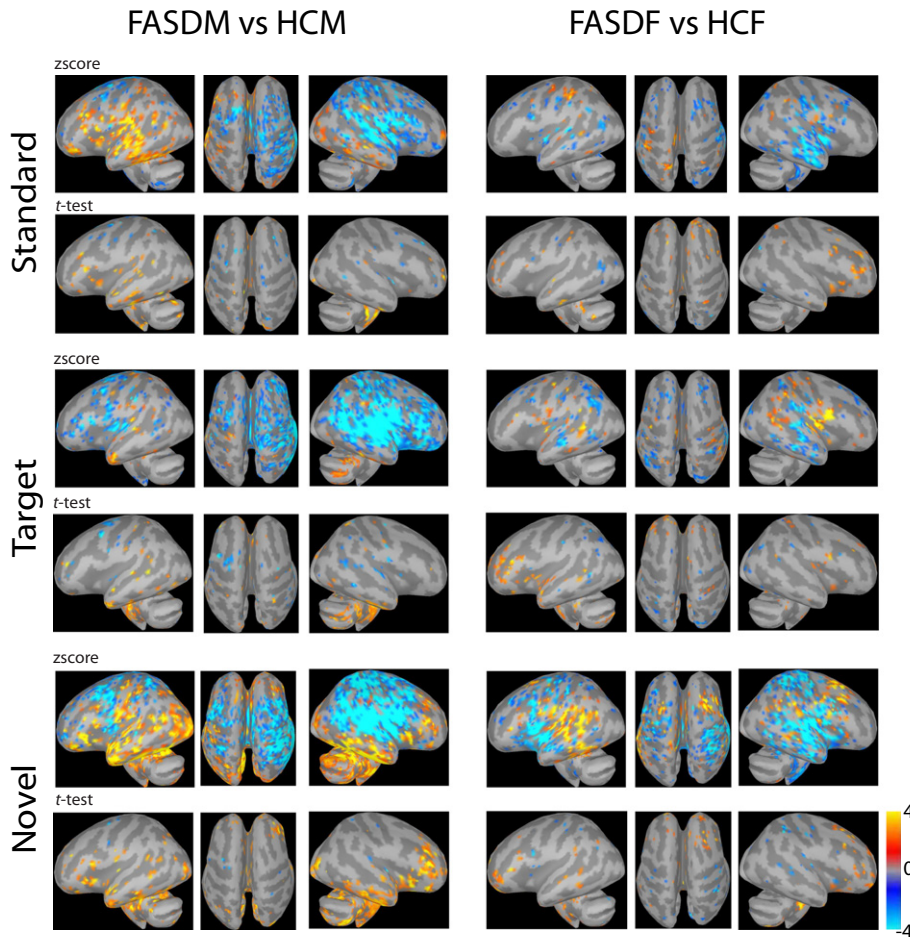
Fig. 7. Comparison of group-averaged brain activation patterns for FASD vs. age- and sex-matched healthy controls at 250 ms following presentation of the standard, target and novel stimuli. The z-score plots show the difference of the mean brain activation for FASDM vs. HCM and for FASDF vs. HCF. The absolute values of the current flow at each location were normalized for each individual participant to the baseline activation from 500 to 0 ms before stimulus presentation. The corresponding t-test plots were thresholded at $p < 0.05$.

FASDM vs HCM   FASDF vs HCF
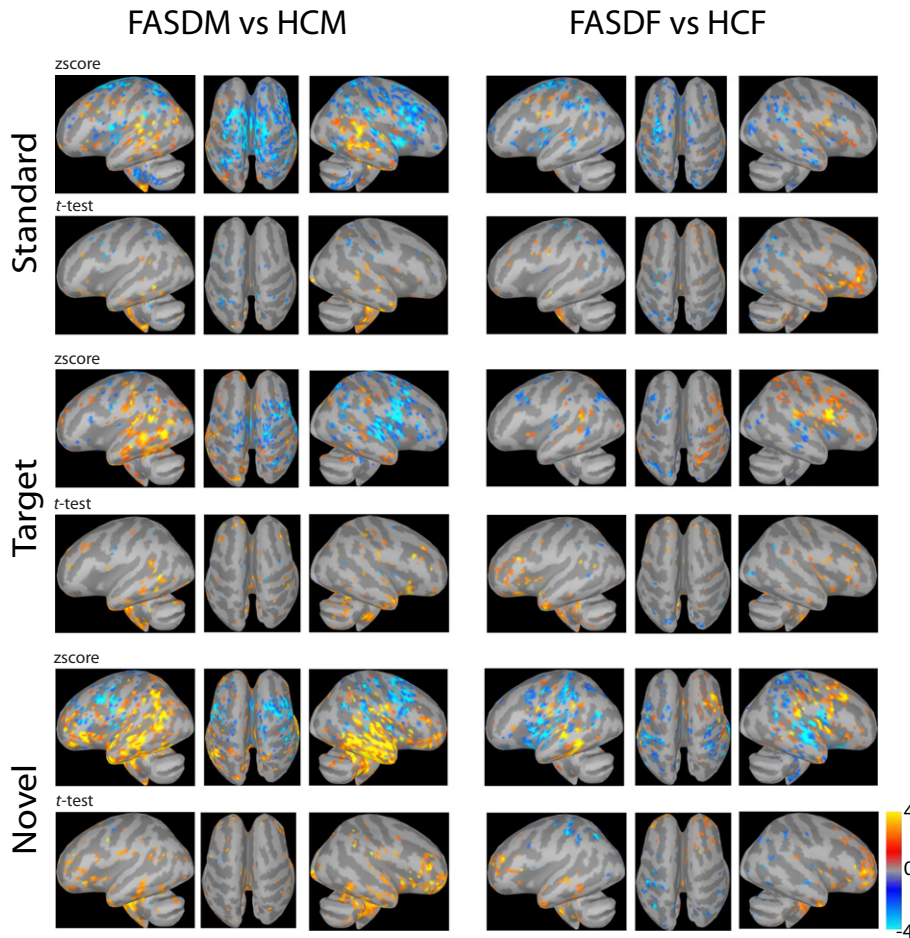
Fig. 8. Comparison of group-averaged brain activation patterns for FASD vs. age- and sex-matched healthy controls at 350 ms following following presentation of the standard, target and novel stimuli. The z-score plots show the difference of the mean brain activation for FASDM vs. HCM and for FASDF vs. HCF. The absolute values of the current flow at each location were normalized for each individual participant to the baseline activation from 500 to 0 ms before stimulus presentation. The corresponding t-test plots were thresholded at $p < 0.05$.

black bars on the horizontal axes of the figures. The time–frequency plots (Figs. 10, 12, 14) were computed without normalization or thresholding of the results. A matched-pair (sex and age) t-test was used for comparison between groups with p-value threshold of 0.05.

3. Results

3.1. Neuropsychological and behavioral measures

Five participants did not complete the cognitive assessment. The remaining 39 participants (46.15% male) were assessed for a relationship between response time to target auditory stimuli and demographic (age, sex) and cognitive measures (IQ, WASI vocabulary, WASI matrix reasoning). Descriptive statistics and effect sizes can be found in Table 1. No significant between-group differences were detected for age ($t(44) = 0.919$, $p = .36$) or sex ($\chi^2(1, n = 39) = 0.022$, $p = .882$). Large and significant differences were detected for IQ mainly due to a substantial difference in vocabulary (see Table 2). In addition, a significant association was detected between WASI vocabulary and response time ($r = -.350$, $p = .039$). There was no significant effect of sex on response time (RT), the number of false positives, the ratio of incorrect/correct, on RT weighted by hits or on the change of RT or false positives across the 4 blocks. The between group differences were further compared by sex. Significant differences in IQ and vocabulary scores were also observed in male and female group comparisons. In the male comparisons by group, IQ scores were significantly different [$t(15) = 4.42$, $d = 2.28$, $p = 0.001$], with the control males having

higher IQ scores. Vocabulary scores were also significantly different [$t(15) = 5.97$, $d = 3.08$, $p = 0.00003$], with the control males having higher Vocabulary scores. The female comparisons followed the same trend with IQ scores being significantly different [$t(22) = 4.27$, $d = 1.82$, $p = 0.0003$], with the control females having higher IQ scores. Vocabulary scores were also significantly different [$t(21) = 4.53$, $d = 1.98$, $p = 0.0002$], with the control females having higher Vocabulary scores. Again no differences were detected for WASI matrix reasoning, RT, or age. Within group comparisons did not reveal any significant differences between sexes for any of the measures.

3.2. Auditory P50m and N100m latencies

The P50m and N100m peak latencies and the onset of the N100m for the standard stimuli were determined for each participant from waveforms for activity in primary/secondary auditory cortex (Fig. 1a). An independent samples t-test for P50m and N100m latencies and for the N100m onset in the left and in the right hemisphere revealed significant differences between FASD and HC in the left N100m onset [$t(36) = 2.267$, $p = 0.029$, $d = 0.735$] and left N100m latency [$t(39) = 2.368$, $p = 0.023$, $d = 0.739$]. No significant differences were found in the right hemisphere. A Repeated Measures ANOVA was performed to compare the latencies of the P50m, N100m, and N100m evoked responses in the left and right hemisphere. This yielded a significant difference between hemispheres [$F(1,34) = 5.382$, $p = 0.026$, partial $^2 = 0.195$]. FASD latencies were shorter for P50m and N100m compared to healthy controls.

Both FASD and HC showed differences in latency that depended on sex (Fig. 1b). An independent samples t-test revealed that in HC, males and females were significantly different for the left hemisphere N100m onset [$t(17) = 4.137\ p = 0.001$, $d = 1.922$], left hemisphere N100m latency {$t(18) = 3.536\ p = 0.002$, $d = 1.613$}, right hemisphere P50m latency [$t(17) = 2.448$, $p = 0.026$, $d = 1.137$], and right hemisphere N100m latency [$t(19) = 2.834$, $p = 0.011$, $d = 1.273$]. In FASD, males and females were significantly different for the left hemisphere N100m onset [$t(17) = 2.275$, $p = 0.036$, $d = 1.082$], right hemisphere P50m latency [$t(16.151) = 5.905$, $p = 0.000021$, $d = 2.743$], and right hemisphere N100m onset [$t(9) = 2.790$, $p = 0.021$, $d = 1.69$]. However, an independent t-test comparison of female FASD and female HC revealed no significant differences. An independent t-test comparison of male FASD and male HC revealed significant differences in the left hemisphere N100m onset [$t(13) = 2.537$, $p = 0.025$, $d = 1.313$], and left hemisphere N100m latency [$t(14) = 2.229$, $p = 0.043$, $d = 1.115$].

Lateralization differences were observed in HC and tested using paired-sample t-tests. Onset of N100m in the left hemisphere at 72 ms lagged onset in the right at 66 ms [$t(15) = 2.199$, $p = 0.044$, $d = 0.55$]. N100m latency on the left at 100 ms lagged the right at 91 ms [$t(19) = 3.158$, $p = 0.005$, $d = 0.706$]. The difference between the left P50m at 52 ms was almost significant compared to the right P50m at 47 ms [$t(16) = 1.95$, $p = 0.069$, $d = 0.472$]. In contrast no significant differences were observed between the hemispheres in P50m/N100m latency and N100m onset in FASD.

Correlations between the P50m, N100m onset and N100m component latency and neuropsychological tests (WASI: IQ score, Vocabulary, and Matrix Reasoning) were also investigated. No significant correlations were found with the Control males, FASD males, nor with all male scores grouped together. With all female scores combined, there were no significant correlations found with the left or right P50m. There was a correlation between the left N100m latency and IQ [$r(21) = 0.427$, $p = 0.042$, $r^2 = 0.18$] and with the left N100m latency and Matrix Reasoning [$r(20) = 0.459$, $p = 0.032$, $r^2 = 0.21$]. There was also a correlation between the right N100m latency and Vocabulary [$r(13) = 0.522$, $p = 0.046$, $r^2 = 0.27$], but not with the left N100m latency. No correlations were found with the Control or FASD females. There were also no correlations found in the combined control group. In the FASD group, there were no correlations with the left and right P50m and N100m onset. There was a correlation between the right N100m and Vocabulary [$r(14) = -0.512$, $p = 0.043$, $r^2 = 0.26$], but not in the left N100m.

3.3. Evoked-response MEG sensor waveforms

Fig. 2 shows group-averaged MEG sensor waveforms and global field power (GFP) for standard, target and novel trials. A prominent N100m evoked-response peak is visible at ~100 ms. There are also a series of peaks from 250 to 450 ms for standard, target and novel trials, and also sustained activity to 800 and 1000 ms for target and novel trials, respectively.

3.4. Brain activation patterns

Figs. 3–5 show group-averaged patterns of brain activation represented on the cortical surface as the absolute value of current flow at 0, 100, 250 and 350 ms following presentation of the standard, target and novel stimuli. Responses for standard stimuli were strongly right lateralized for both FASDM and HCM but not for FASDF and HCF at 100, 250 and 350 ms. Increased frontal and parietal activation was seen at 100 ms for both FASDM and FASDF. Responses following target stimuli showed a similar pattern of strongly right-lateralized activation for FASDM and HCM, but not for FASDF and HCF. Increased frontal and parietal activation for FASDM and FASDF was seen at 100 and also
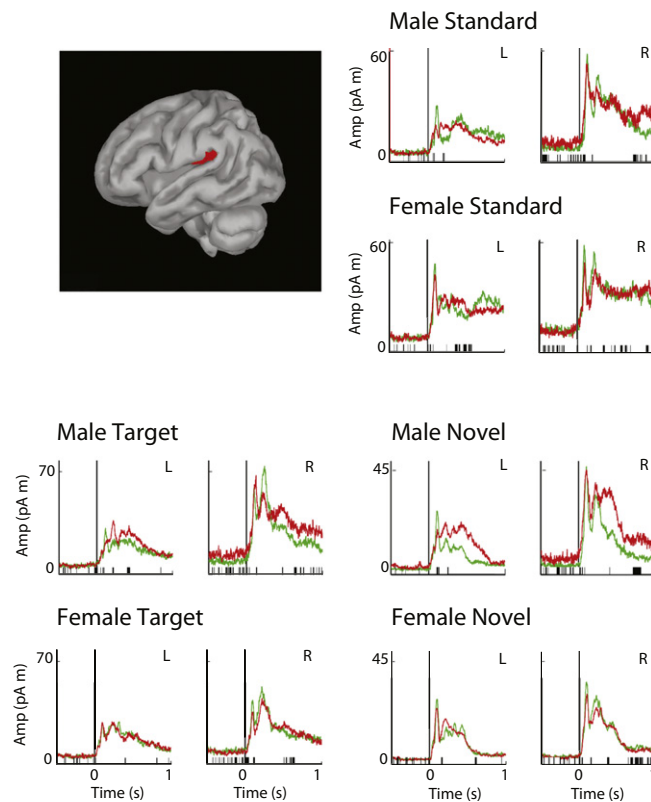
Fig. 9. Group-averaged brain activity in and near the primary auditory cortex for standard, target and novel stimuli. The MR image shows the region of interest centered on the posterior ramus of the lateral sulcus. The waveforms show the absolute value of the current flow in picoAmp meter (pAm) as a function of time averaged over all trials. Stimulus onset is at t = 0 ms. Waveforms in the left (L) and right (R) auditory cortex for FASDM and FASDF are shown in red and for HCM and HCF in green. The black dashed lines above the x-axes show epochs of significant differences between the waveforms in each figure.

350 ms. Responses following novel stimuli showed right-lateralized activation for all groups, with frontal activation at 100 ms and temporal activation at 350 ms for FASDM.

Figs. 6–8 show group-averaged patterns of brain activation for FASDM vs. HCM and FASDF vs. HCF at 0, 100, 250 and 350 ms following presentation of the standard, target and novel stimuli. The data for each of the participants were normalized to baseline values (from 500 to 0 ms before stimulus presentation) prior to computation of the mean activation patterns for each group. Thus Figs. 6–8 reflect both activation at the indicated time epochs and also baseline activation levels.

In Fig. 6, the t-test plots at 100 ms reveal scattered regions of significant differences between FASDM and HCM, including increased activation of the right parietal cortex for standard stimuli and of the right cerebellum for target stimuli in FASDM. Novel stimuli

elicited significant increases in bilateral frontal, parietal and cerebellar cortex for FASDM compared to HCM. There was also increased activation of bilateral frontal cortex in FASDF compared to HCF for all three stimulus types.

In Fig. 7 the t-test plots at 250 ms reveal significant increases for FASDM in left temporal and left inferior frontal activation and decreases in bilateral medial frontal and right frontal activation compared to HCM for standard stimuli. Responses for target stimuli also showed significant increases in left temporal activation and decreases in bilateral medial frontal and right frontal activation. Novel stimuli elicited significant increases in bilateral temporal and frontal activation. There was also significant increases for FASDF in bilateral frontal activation to standard stimuli, right frontal activation to target stimuli and bilateral activation to novel stimuli compared to HCF. Novel stimuli also elicited increases
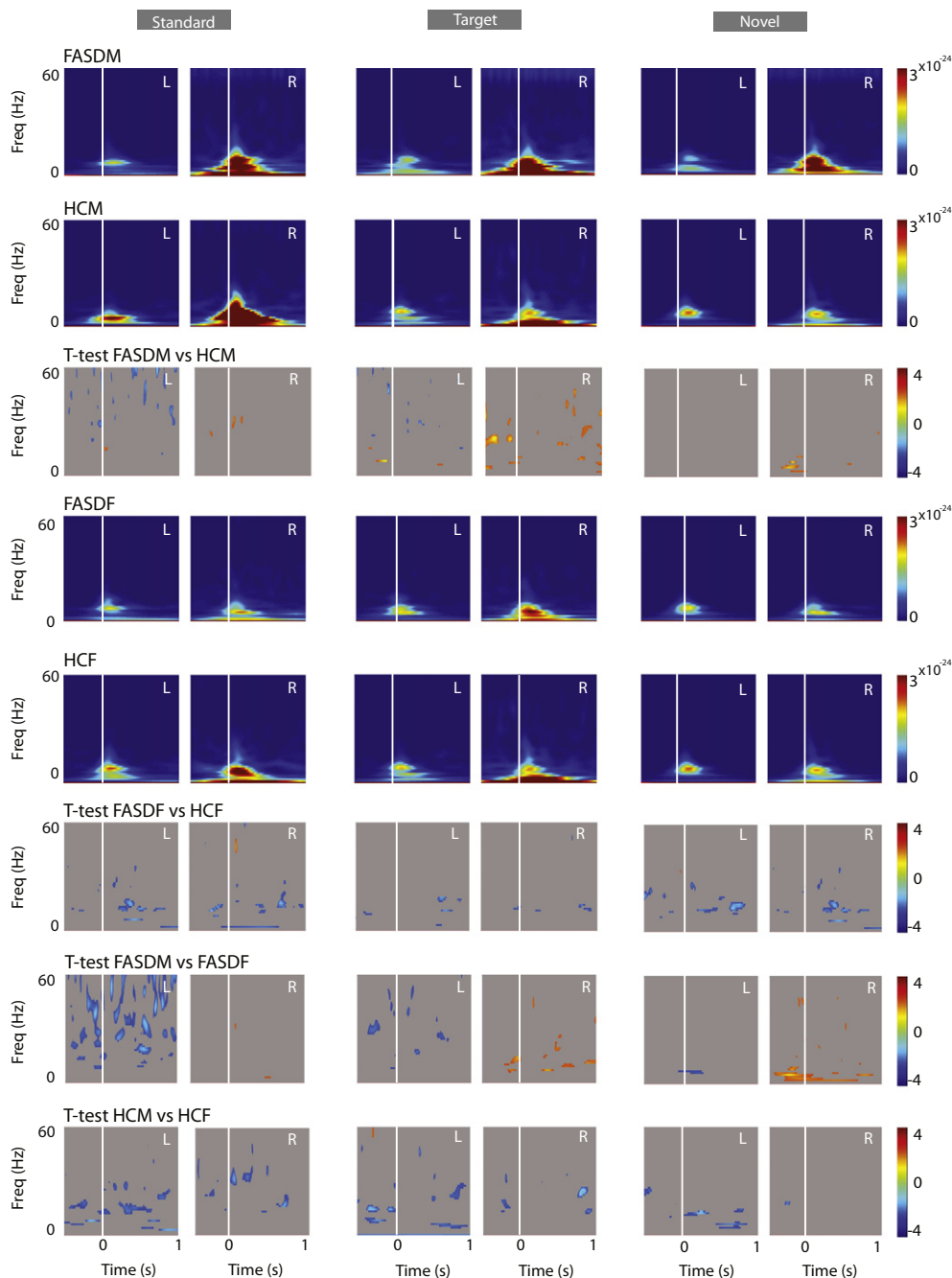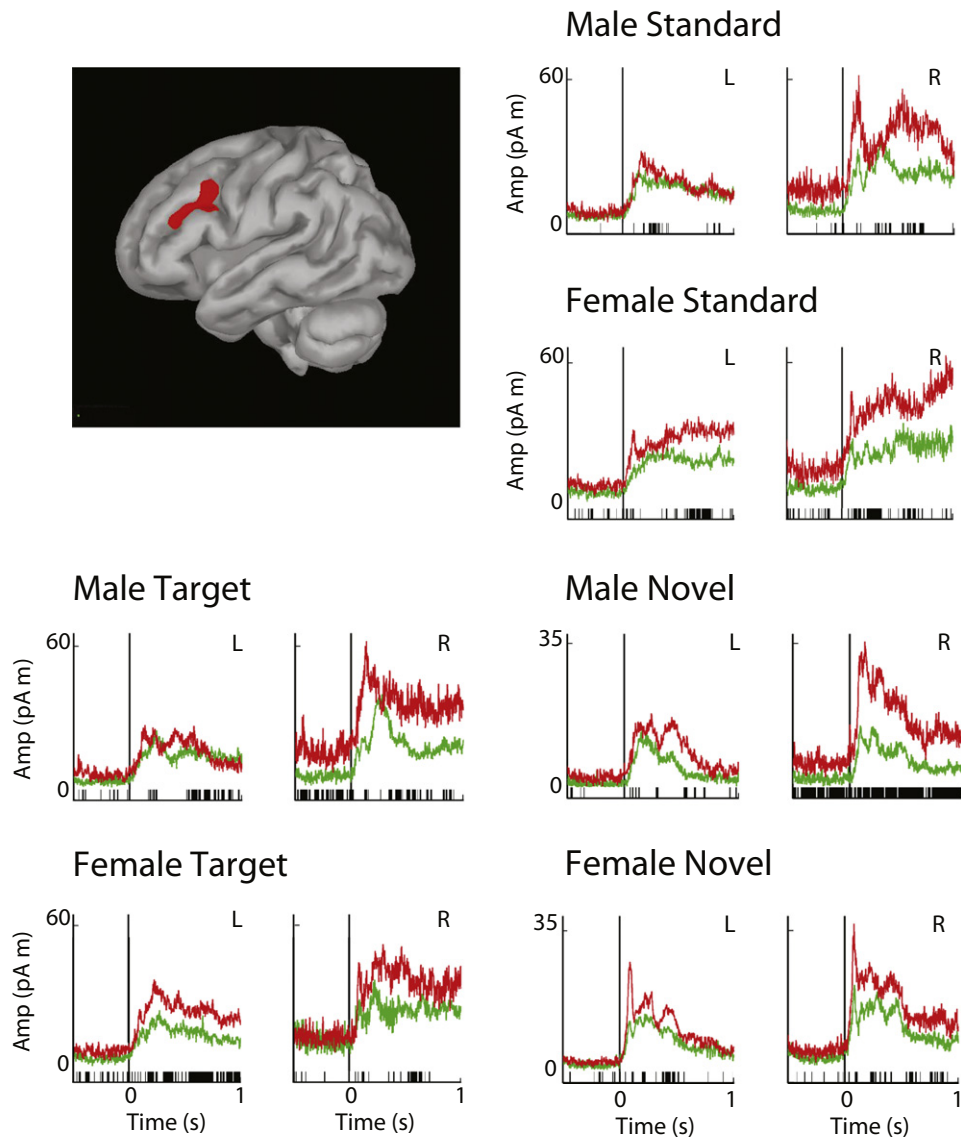

Fig. 10. Power time–frequency plots of the group-averaged current flow for FASDM, HCM, FASDF and HCF in and near the left (L) and right (R) primary auditory cortex for standard, target and novel stimuli in picoAmp meter^2. Stimulus onset is at t = 0 ms. The paired t-test plots show significant differences between groups.

Fig. 11. Group-averaged brain activity in and near the inferior frontal sulcus for standard, target and novel stimuli. The MR image shows the region of interest. The waveforms show the absolute value of the current flow in picoAmp meter (pAm) as a function of time averaged over all trials. Stimulus onset is at t = 0 ms. Waveforms in the left (L) and right (R) auditory cortex for FASDM and FASDF are shown in red and for HCM and HCF in green. The black dashed lines above the x-axes show epochs of significant differences between the waveforms in each figure.

in medial frontal and decreases in parietal activation in FASDF compared to HC. Both target and novel stimuli elicited significant increases in the cerebellum for FASDM compared to HCM, but not for FASDF compared to HCF.

In Fig. 8 the *t*-test plots at 350 ms for standard stimuli show significant decreases in bilateral frontal and parietal cortex and increases in bilateral temporal cortex for FASDM compared to HCM. Target and novel stimuli elicited significant increases in bilateral frontal and temporal cortex for FASDM. There were also significant increases in right frontal activation to standard stimuli and increases in bilateral frontal activation to target and novel stimuli for FASDF compared to HCF. Decreased activation of bilateral parietal cortex was seen in FASDF for all three stimulus types.

3.5. Brain source waveforms and time–frequency plots

Figs. 9–14 show group-averaged waveforms and power time–frequency (TF) plots for current flow within and near the left and right primary auditory cortex (posterior ramus of the lateral sulcus), the inferior

frontal sulcus and the hippocampus for the standard, target and novel conditions.

Current flow in auditory cortex is shown in Fig. 9. Although there are intermittent epochs of significant differences between FASD and HC both before and after stimulus presentation, differences in the amplitude of the N100m response to standard and target stimuli are not significant. Interestingly, the evoked-response waveforms following standard and target stimuli reveal sustained activity from 0.5 to 1 s for both FASD and HC. The activity at 1 s occurs just prior to the earliest possible presentation of a subsequent stimulus. In contrast, HCM, HCF and FASDF waveforms for novel trials return to baseline in the left and right hemispheres during the same epoch. Only waveforms for FASDM show a tendency for sustained activity in the right hemisphere.

The TF plots in Fig. 10 for current flow in the auditory cortex reveal stimulus-locked alpha-band (8–13 Hz) activity for both FASD and HC. Right-lateralization of responses is seen for HCM for standard stimuli and for FASDM for all stimulus types. Right-lateralization of responses for standard stimuli is seen also for HCF, and for target stimuli for FASDF. The *t*-test plots for the right auditory
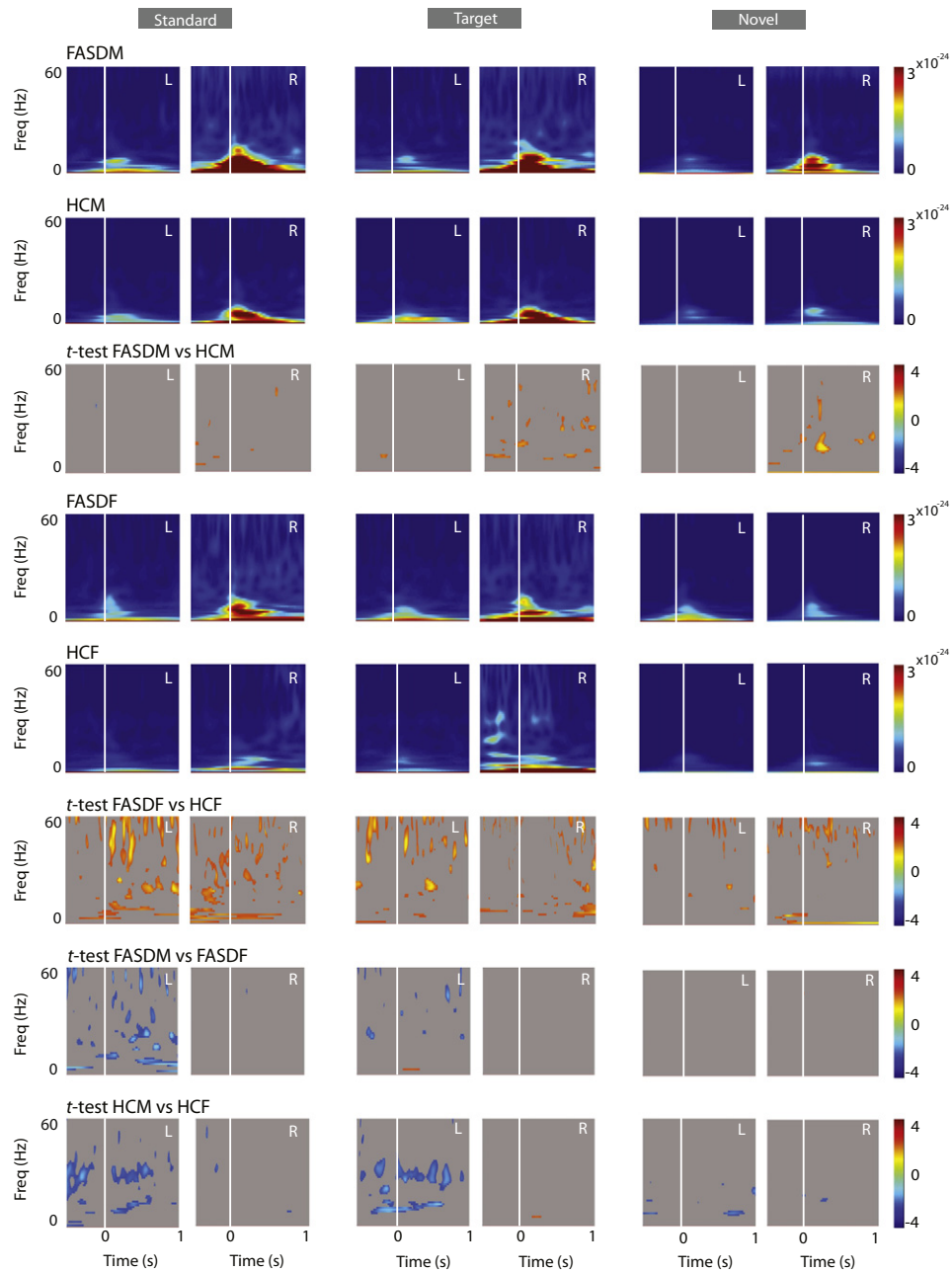
Fig. 12. Power time–frequency plots of the group-averaged current flow for FASDM, HCM, FASDF and HCF in and near the left (L) and right (R) inferior frontal sulcus for standard, target and novel stimuli in picoAmp meter^2. Stimulus onset is at t = 0 ms. The paired *t*-test plots show significant differences between groups.

cortex show significant increases in alpha-band activity for FASDM compared to HCM both prior to and after stimulus presentation for target stimuli. In contrast, the *t*-test plots for FASDF vs. HCF show significant decreases in alpha-band activity for FASDF both prior to and after stimulus presentation in the left and right auditory cortex for all stimulus types. The *t*-test plots for standard trials in the left but not the right auditory cortex also show significant increased alpha, beta (13–35 Hz) and gamma (35–60 Hz) activities for FASDM compared to FASDF. Increased gamma-band activity in the left auditory cortex is not seen in HCM vs. HCF. The *t*-test plots for the right auditory cortex show significant increased alpha-band activity for FASDF compared to FASDM for target stimuli.

Fig. 11 shows waveforms for current flow in the inferior frontal sulcus. In contrast to the waveforms for activity within the left and right auditory cortex, Fig. 11 reveals multiple epochs of significant

differences between responses for FASD compared to HC, with amplitudes for FASD exceeding that for HC for all stimulus categories, particularly in the right hemisphere. There is also sustained activity from 0.5 to 1 s following standard and target stimuli for FASD and HC, and sustained activity from 0.5 to 1 s in the right inferior frontal sulcus following novel stimuli for FASD. Significant differences in baseline activity are also seen in the data for both male and female FASD compared to controls.

The TF plots in Fig. 12 for current flow in the inferior frontal sulcus are similar to those for the auditory cortex, in that stimulus-locked alpha-band activity is more right-lateralized for both FASD and HC following standard and target stimuli. In contrast to the results for the auditory cortex, alpha-band activity for novel stimuli is more right-lateralized for FASDM and more left lateralized for FASDF. The *t*-test plots show significantly increased alpha-band activity for FASDM
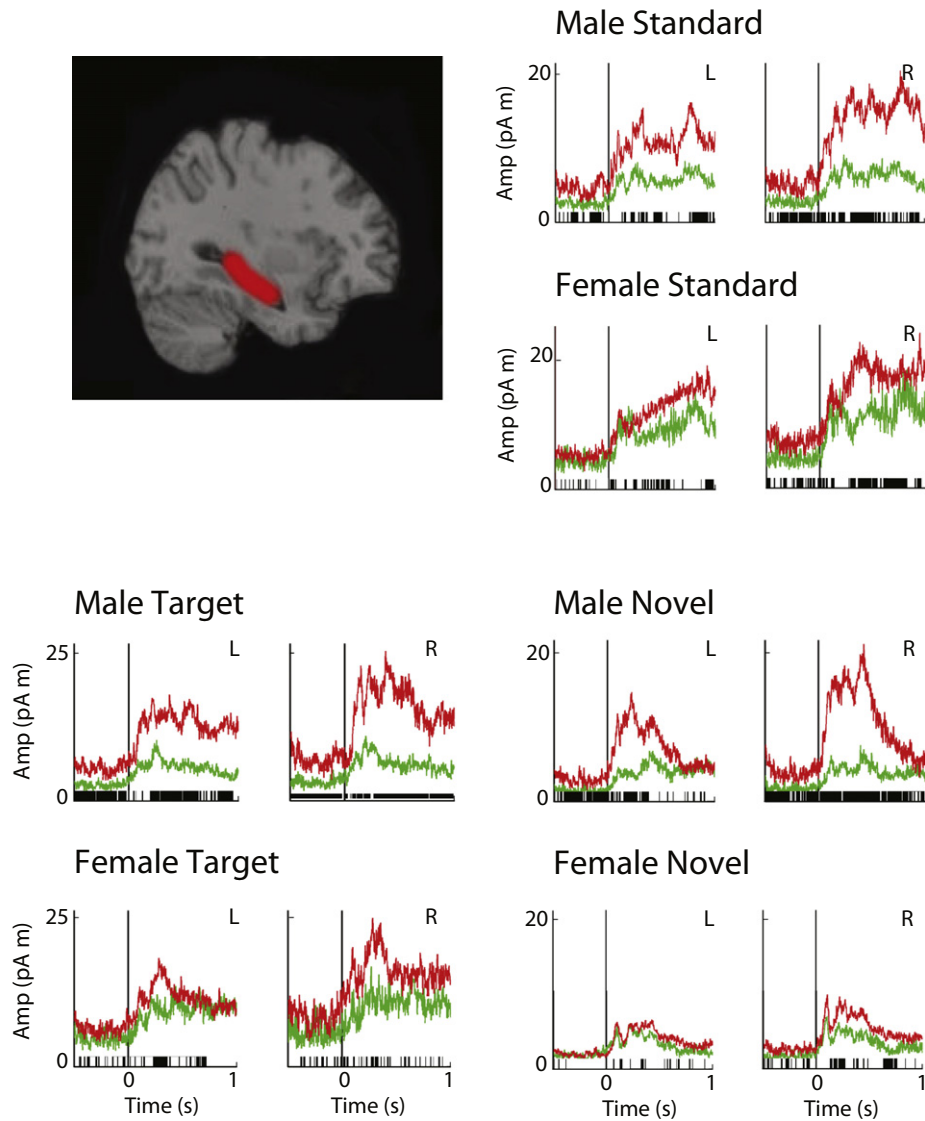
Fig. 13. Group-averaged brain activity in and near the hippocampus for standard, target and novel stimuli. The MR image shows the region of interest. The waveforms show the absolute value of the current flow in picoAmp meter (pAm) as a function of time averaged over all trials. Stimulus onset is at t = 0 ms. Waveforms in the left (L) and right (R) auditory cortex for FASDM and FASDF are shown in red and for HCM and HCF in green. The black dashed lines above the x-axes show epochs of significant differences between the waveforms in each figure.

compared to HCM both prior to and after stimulus presentation in the right inferior frontal sulcus for target and novel stimuli. In contrast to the results for the auditory cortex, the *t*-test plots for FASDF vs. HCF for standard stimuli show significant increases in alpha-, beta- and gamma-band activities for FASDF after stimulus presentation in the left hemisphere and both prior to and after stimulus presentation in the right hemisphere. Gamma-band increases for FASDF compared to HCF can also be seen for target and novel trials. The *t*-test plots for FASDM vs. FASDF for standard and target trials show decreased alpha-, beta- and gamma-band activities in the left hemisphere for male compared to female FASD. The *t*-test plots for HCM vs. HCF for standard and target trials also show decreased alpha- and beta-band activities in the left hemisphere for males compared to female HC. In contrast to responses in the auditory cortex, there are few significant differences for either FASDM vs. FASDF or for HCM vs. HCF in the right hemisphere for standard and target stimuli, or in either hemisphere for novel stimuli.

Fig. 13 shows waveforms for current flow in and near the hippocampus. There are multiple epochs of significant differences between

responses for FASD compared to HC, with waveform amplitudes for FASD exceeding that for HC for all stimulus categories in both the left and right hemispheres. FASDM waveforms show a pronounced, bilateral and prolonged P300-type response to novel stimuli with a sustained response to ~800 ms. There are also significant differences between FASD and HC in the sustained activity from 0.5 to 1 s following standard and target stimuli. Differences in baseline activity are also seen in the data for all conditions with the exception of the left hemisphere responses in the hippocampus for FASDF compared to HCF.

The TF plots in Fig. 14 for current flow in and near the hippocampus show increased bilateral alpha-band activity for FASDM compared to HCM following standard and target stimuli, and increased right-hemisphere alpha-band activity following novel stimuli. Differences in the TF plots for FASDF and for HCF are less pronounced, although interesting stimulus-locked beta- and gamma-band activities can be seen for both FASDF and HCF. The *t*-test plots for FASDM vs. HCM for standard and target stimuli reveal significant increases in alpha-, beta- and gamma-band activities for FASDM. Alpha-band
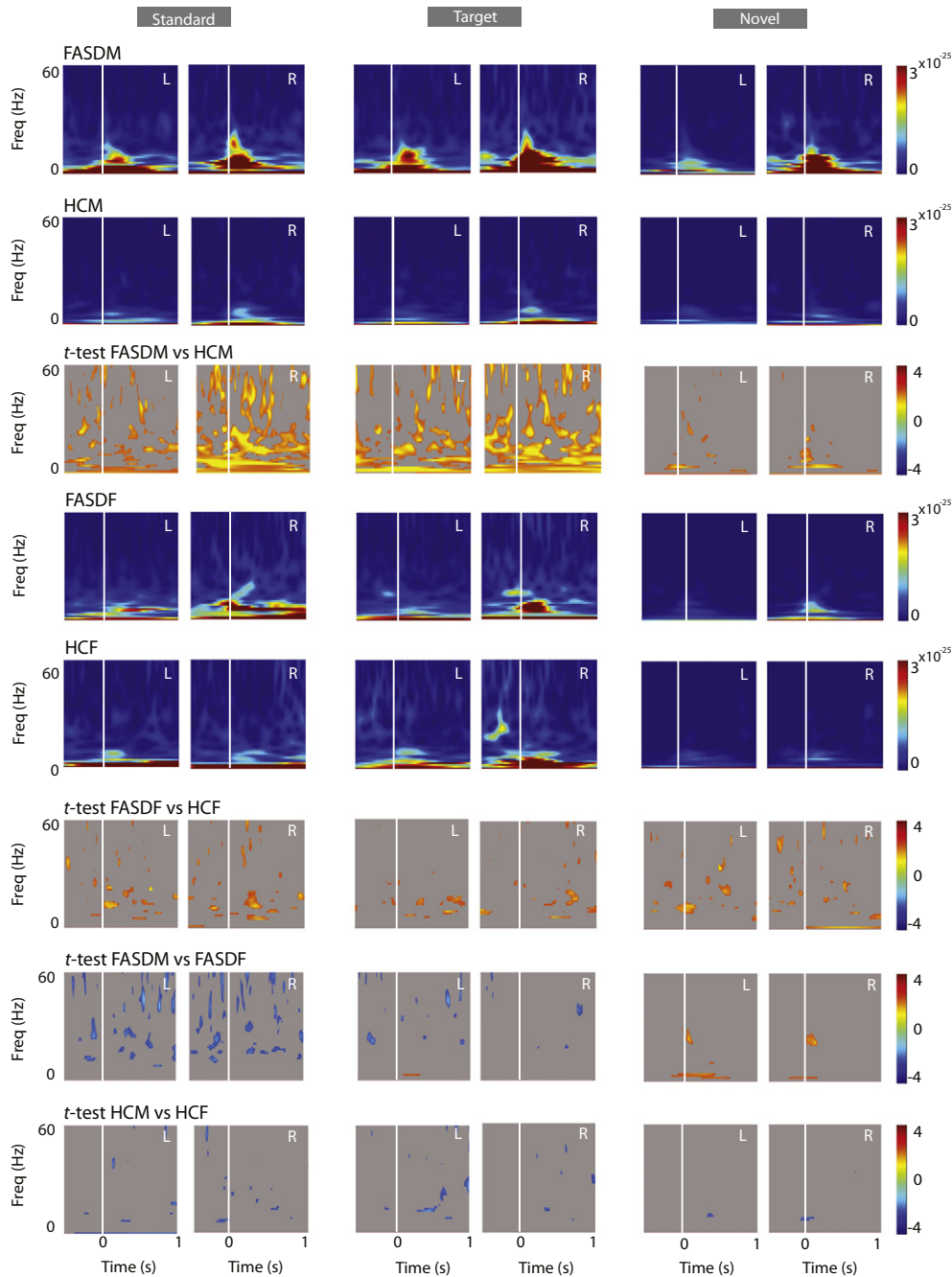
Fig. 14. Power time–frequency plots of the group-averaged current flow for FASDM, HCM, FASDF and HCF in and near the left (L) and right (R) hippocampus for standard, target and novel stimuli in picoAmp meter^2. Stimulus onset is at t = 0 ms. The paired *t*-test plots show significant differences between groups.

activity is also significantly increased for FASDF compared to HCF, although the differences are not as pronounced. The *t*-test plots for standard stimuli also reveal significantly less alpha-, beta- and gamma-band activation for FASDM compared to FASDF in the left and right hippocampus, but only minor differences for HCM compared to HCF.

4. Discussion

The present study revealed differences in brain activation and dynamics in adolescents with FASD compared to typically-developing controls during the performance of an auditory oddball task. This task probes development of top-down perceptual expectation for repeated

(standard) tones, detection of target tones that elicit a behavioral response and processing of novel digital sounds in cortico-hippocampal circuits (Halgren et al., 1998). The main finding was widespread sex-specific differential activation of the frontal and medial temporal cortex in adolescents with FASD compared to typically developing controls. Significant differences in evoked-response and time–frequency measures of brain dynamics for FASD were observed for all stimulus types in the auditory cortex, inferior frontal sulcus and hippocampus. These results underscore the importance of considering the influence of sex when analyzing neurophysiological data in children with FASD.

Although FASD responded more slowly to target tones compared to HC in the oddball task, there was no effect of sex on the response times to target stimuli. In contrast, significant differences were observed in

the latencies of the auditory N100m response to standard stimuli between male and female participants with FASD. In a previous MEG study of 10 preschool children with FASD and 15 healthy controls, Stephen and colleagues (2012) found significant delays in FASD in the N100m and N200m evoked-response peaks following presentation of a train of 1000 Hz tone bursts. This interesting study suggested that auditory evoked-response latency differences may evidence alcohol-induced brain damage in this age group. In the present study on 22 adolescents with FASD and 22 typically developing controls, latency differences between participants with FASD and healthy controls were observed in both the P50m and N100m auditory evoked responses. In contrast to the Stephen study, latencies of the P50m and N100m were shorter for adolescent FASD compared to healthy controls. An earlier EEG auditory oddball study by Kaneko et al. (1996a) reported no significant N100 latency differences for standard stimuli between children from 4 to 15 years with FAS and healthy controls. Stephen et al. suggested that the discrepancy between their results and that of Kaneko et al. may be due in part to maturational differences in auditory processing between younger and older children. Maturation of the cortical auditory evoked response in typically developing children is known to shorten the latency of N1 and P2 in EEG scalp recordings (Wunderlich et al., 2006). In the context of FASD, studies performed in alcohol-exposed rats reveal that abnormalities in auditory brainstem responses observed in the newborn (Church, 1987) tend to dissipate in adulthood (Church et al., 2012; Leigland et al., 2013). Taken together, these data suggest that, although neurophysiological measures of auditory processing delays may have potential as markers for compromised brain function in very young children with FASD, these measures may not be useful for older children.

Another possible contributor to the observed differences between the young children in prior work (Kaneko et al., 1996a; Stephen et al., 2012) and the present study could be in the nature of the auditory stimuli presented to each group. The young children in the Stephen study were passively exposed to trains of 1000 Hz tones. Children in the Kaneko study listened to standard, rare and noise-burst stimuli but did not make a behavioral response, In contrast, adolescents in the present oddball study were requested to make a motor response to the (rare) target stimuli. Thus our task probed not only development of a "top-down" perceptual expectation for the repeated standard tones and processing of novel digital sounds in cortico-hippocampal circuits but also generation of behavioral responses to target tones and inhibition of behavioral responses to both standard and novel stimuli. Thus participants needed to attend to all of the oddball stimuli in order to successfully perform the requested motor response. Stimulus-driven attention is known to increase the speed of auditory processing (Folyi et al., 2012). Hence the latency differences observed for the standard stimuli between FASD and HC in the present oddball study may reflect not just maturation but also a contribution from differences in "top down" attentional and inhibitory functions between the two groups. In support of this notion, we observed widespread activation, not only of auditory, but also of frontal cortex as early as 100 ms after stimulus presentation. Activation of the frontal cortex continued until immediately prior to presentation of the subsequent stimuli with significant differences in brain activation between male and female FASD and sex-matched HC.

The shorter P50m and N100m auditory evoked-response latencies in the auditory cortex in FASD did not translate into reduced response times to the target stimuli. This result supports the notion that, although differences in early processing in the auditory cortex may evidence the effects of alcohol exposure in FASD, processing in other cortical and/or subcortical regions must also have been impacted by alcohol exposure. Prenatal ethanol exposure is known to affect both the frontal cortex and hippocampus (for a review, see Roussotte et al., 2010), and also to produce sex-specific deficits in the hippocampus in rodent models (Coleman et al., 2012; Sickmann et al., 2014). Our results indicate that the application of high-temporal-resolution neuroimaging techniques such as MEG with the potential to characterize brain dynamics in

frontal-hippocampal circuitry can play a valuable role in characterizing neurophysiological deficits seen in FASD.

In the present study, significant differences were observed between FASD and HC and between males and females in the evoked-response waveforms and in the time–frequency (TF) plots of stimulus-locked oscillatory activity for regions of interest centered in the primary/secondary auditory cortex, inferior frontal sulcus and hippocampus. Although the relationship between evoked-response waveforms, ongoing (endogenous) alpha, induced (stimulus-locked) alpha and stimulus-evoked alpha in MEG data are complex and controversial (for a review, see Mazaheri and Jensen, 2010), oscillatory activity is believed to play a critical role in the sculpting and coordination of brain function. Alpha-band (8–13 Hz) activity has been implicated in timing and attention (for a review see Klimesch, 2012) and in the inhibition of neuronal populations irrelevant to task performance (Jensen and Mazaheri, 2010). Although alpha oscillations can be found throughout the frontal and posterior cortex, the most prominent alpha-band activity (eyes-closed alpha) occurs near the parieto-occipital sulcus in the absence of visual stimuli. Reduction of left-hemisphere eyes-closed alpha has been reported in a previous EEG study in FAS (Kaneko et al., 1996b).

MEG detection of stimulus-induced alpha in the auditory cortex (tau) has been reported by several groups (Tiihonen et al., 1991; Lehtelä et al., 1997; for a review, see Weisz et al., 2011). In the present study, differences between FASD and HC and between males and females were more apparent in the stimulus-locked alpha-band activity than in the evoked-response waveforms. The significant increases in the alpha-band activity seen in the left hemisphere for HCF compared to FASDF, for FASDF compared to FASDM and for HCF compared to HCM suggest that measures of induced alpha may be salient markers for abnormalities in inhibitory processes in the auditory cortex in FASD.

The motivation for selecting the inferior frontal sulcus as a region of interest in the present study is the known role of the ventrolateral prefrontal cortex (VLPFC) in the processing of acoustic features of complex sounds (for a review, see Plakke and Romanski, 2014). Auditory association areas, including the auditory belt and superior temporal gyrus project to VLPFC areas 12/47, 45, and 12 orbital. A more general role of the right inferior frontal cortex in auditory processing is somewhat more controversial (cf. Swick and Chatham, 2014; Aron et al., 2014), although recent fMRI data suggest that inferior frontal cortical regions participate to spatially distributed networks in the processing of infrequent stimuli (Erika-Florence et al., 2014).

In the present study, in contrast to responses seen in the auditory cortex, there was a consistent increase in evoked-response and alpha-band activity in the inferior frontal sulcus for standard and target stimuli in FASD compared to HC. In male FASD, increases were seen primarily in the right hemisphere. In female FASD, increased activity was more bilateral and accompanied by prominent right-hemisphere gamma oscillations. A deficit in inhibitory interneuron development, hypothesized to be a long-term consequence of developmental ethanol exposure (Sadrian et al., 2013), may contribute to this increased evoked-response, alpha- and gamma-band activities seen in FASD.

In pioneering passive oddball EEG study of children with FAS, Kaneko, Riley and collaborators found latencies of the P300 evoked response over the parietal cortex to novel stimuli to be increased in FAS compared to controls (Kaneko et al., 1996a). The oddball paradigm in the EEG literature is utilized to characterize attention and novelty detection, with the P3a component of the P300 associated with involuntary orientation of attention to novel stimuli in fronto-hippocampal circuits, and the P3b component associated with voluntary detection of task-salient target stimuli (for a review see Soltani and Knight, 2000; Polich, 2007). In the present MEG study, significant differences emerged between FASD and HC in and near the hippocampus. Standard, target and novel stimuli all elicited significant increases in evoked-response amplitudes in FASD compared to HC at 300 ms, with sustained activation to 1000 ms for both standard and target, but not novel, stimuli. TF

plots revealed increased alpha, beta and gamma-band activities for FASD vs. HC and for FASDM vs. FASDF for standard and target stimuli, and for FASDF vs. HCF for novel stimuli. The elevated activation to all stimulus types was also seen in the right inferior frontal sulcus in FASD. Hyperactivity has been reported in olfacto-hippocampal circuits in the alcohol-exposed rodent during both the spontaneous (resting) state and in sensory-evoked responses (Wilson et al., 2011). Although a detailed analysis of cortico-hippocampal network dynamics is not reported here, these results suggest a common auditory-evoked and alpha-band hyperactivity in both the inferior frontal sulcus and hippocampus in adolescents with FASD. Observation of both evoked-response and alpha-band differences in FASD enlarges the potential set of neurophysiological measures for the impact of alcohol exposure on brain function.

5. Conclusions

The main finding of this MEG study was widespread sex-specific differential activation of the auditory, frontal and mesial temporal cortex in adolescents with FASD compared to typically developing controls during the performance of an auditory oddball task. This task probed development of top-down perceptual expectation for repeated (standard) tones, detection of (rare) target tones that elicit a behavioral response and processing of novel digital sounds in cortico-hippocampal circuits. Auditory N100m evoked-response latencies for FASD compared to healthy controls were opposite to those reported previously for very young children. Significant sex-related differences in evoked-response and oscillatory time–frequency measures of brain dynamics were observed for all stimulus types. These results underscore the importance of considering the potential effect of sex when analyzing neurophysiological data in adolescents with FASD and expand the potential set of neurophysiological markers for this disorder.

Conflict of interest

The authors declare no competing financial interests.

Acknowledgments

References

Abel, E.L., Sokol, R.J., 1986. Fetal alcohol syndrome is now leading cause of mental retardation. Lancet 2 (8517), 1222. http://dx.doi.org/10.1016/S0140-6736(86)92234-82877359.

Aron, A.R., Robbins, T.W., Poldrack, R.A., 2014. Inhibition and the right inferior frontal cortex: one decade on. Trends Cogn. Sci. 18 (4), 177–185. http://dx.doi.org/10.1016/j.tics.2013.12.00324440116.

Astley, S.J., Olson, H.C., Kerns, K., Brooks, A., Aylward, E.H., Coggins, T.E., Davies, J., Dorn, S., Gendler, B., Jirikowic, T., Kraegel, P., Maravilla, K., Richards, T., 2009. Neuropsychological and behavioral outcomes from a comprehensive magnetic resonance study of children with fetal alcohol spectrum disorders. Can. J. Clin. Pharmacol. 16 (1), e178–e20119329824.

Blakemore, S.J., 2012. Imaging brain development: the adolescent brain. Neuroimage 61 (2), 397–406. http://dx.doi.org/10.1016/j.neuroimage.2011.11.08022178817.

Chudley, A.E., Conry, J., Cook, J.L., Loock, C., Rosales, T., LeBlanc, N., Public Health Agency of Canada's National Advisory Committee on Fetal Alcohol Spectrum Disorder, 2005. Fetal alcohol spectrum disorder: Canadian guidelines for diagnosis. CMAJ 172 (5 Suppl), S1–S21. http://dx.doi.org/10.1503/cmaj.104030215738468.

Church, M.W., 1987. Chronic in utero alcohol exposure affects auditory function in rats and in humans. Alcohol 4 (4), 231–239. http://dx.doi.org/10.1016/0741-8329(87)90017-63620090.

Church, M.W., Hotra, J.W., Holmes, P.A., Anumba, J.I., Jackson, D.A., Adams, B.R., 2012. Auditory brainstem response (ABR) abnormalities across the life span of rats prenatally exposed to alcohol. Alcohol. Clin. Exp. Res. 36 (1), 83–96. http://dx.doi.org/10.1111/j.1530-0277.2011.01594.x21815896.

Coleman Jr, L.G., Oguz, I., Lee, J., Styner, M., Crews, F.T., 2012. Postnatal day 7 ethanol treatment causes persistent reductions in adult mouse brain volume and cortical neurons with sex specific effects on neurogenesis. Alcohol 46 (6), 603–612. http://dx.doi.org/10.1016/j.alcohol.2012.01.00322572057.

Collins, D.L., Zijdenbos, A.P., Kollokian, V., Sled, J.G., Kabani, N.J., Holmes, C.J., Evans, A.C., 1998. Design and construction of a realistic digital brain phantom. IEEE Trans. Med. Imaging 17 (3), 463–468. http://dx.doi.org/10.1109/42.7121359735909.

Destrieux, C., Fischl, B., Dale, A., Halgren, E., 2010. Automatic parcellation of human cortical gyri and sulci using standard anatomical nomenclature. Neuroimage 53 (1), 1–15. http://dx.doi.org/10.1016/j.neuroimage.2010.06.01020547229.

Erika-Florence, M., Leech, R., Hampshire, A., 2014. A functional network perspective on response inhibition and attentional control. Nat. Commun. 5, 4073.

Folyi, T., Fehér, B., Horváth, J., 2012. Stimulus-focused attention speeds up auditory processing. Int. J. Psychophysiol. 84 (2), 155–163. http://dx.doi.org/10.1016/j.ijpsycho.2012.02.00122326595.

Gautam, P., Nuñez, S.C., Narr, K.L., Mattson, S.N., May, P.A., Adnams, C.M., Riley, E.P., Jones, K.L., Kan, E.C., Sowell, E.R., 2014. Developmental trajectories for visuo-spatial attention are altered by prenatal alcohol exposure: a longitudinal FMRI study. Cereb. Cortex http://dx.doi.org/10.1093/cercor/bhu16225092900.

Green, C.R., Lebel, C., Rasmussen, C., Beaulieu, C., Reynolds, J.N., 2013. Diffusion tensor imaging correlates of saccadic reaction time in children with fetal alcohol spectrum disorder. Alcohol. Clin. Exp. Res. http://dx.doi.org/10.1111/acer.1213223551175.

Halgren, E., Marinkovic, K., Chauvel, P., 1998. Generators of the late cognitive potentials in auditory and visual oddball tasks. Electroencephalogr. Clin. Neurophysiol. 106 (2), 156–164. http://dx.doi.org/10.1016/S0013-4694(97)00119-39741777.

Helfer, J.L., White, E.R., Christie, B.R., 2012. Enhanced deficits in long-term potentiation in the adult dentate gyrus with 2nd trimester ethanol consumption. PLOS One 7 (12), e51344. http://dx.doi.org/10.1371/journal.pone.005134423227262.

Hwang, K., Velanova, K., Luna, B., 2010. Strengthening of top-down frontal cognitive control networks underlying the development of inhibitory control: a functional magnetic resonance imaging effective connectivity study. J. Neurosci. 30 (46), 15535–15545. http://dx.doi.org/10.1523/JNEUROSCI.2825-10.201021084608.

Jégou, S., El Ghazi, F., de Lendeu, P.K., Marret, S., Laudenbach, V., Uguen, A., Marcorelles, P., Roy, V., Laquerrière, A., Gonzalez, B.J., 2012. Prenatal alcohol exposure affects vasculature development in the neonatal brain. Ann. Neurol. 72 (6), 952–960. http://dx.doi.org/10.1002/ana.2369923280843.

Jensen, O., Mazaheri, A., 2010. Shaping functional architecture by oscillatory alpha activity: gating by inhibition. Front. Hum. Neurosci. 4, 186–194. http://dx.doi.org/10.3389/fnhum.2010.0018621119777.

Kaneko, W.M., Ehlers, C.L., Philips, E.L., Riley, E.P., 1996a. Auditory event-related potentials in fetal alcohol syndrome and Down's syndrome children. Alcohol. Clin. Exp. Res. 20 (1), 35–42. http://dx.doi.org/10.1111/j.1530-0277.1996.tb01040.x8651459.

Kaneko, W.M., Phillips, E.L., Riley, E.P., Ehlers, C.L., 1996b. EEG findings in fetal alcohol syndrome and Down syndrome children. Electroencephalog. Clin. Neurophysiol. 98 (1), 20–28. http://dx.doi.org/10.1016/0013-4694(95)00189-18689990.

Klimesch, W., 2012. α-band oscillations, attention, and controlled access to stored information. Trends Cogn. Sci. 16 (12), 606–617. http://dx.doi.org/10.1016/j.tics.2012.10.00723141428.

Kodituwakku, P.W., 2009. Neurocognitive profile in children with fetal alcohol spectrum disorders. Dev. Disabil. Res. Rev. 15 (3), 218–224. http://dx.doi.org/10.1002/ddrr.7319731385.

Lebel, C., Roussotte, F., Sowell, E.R., 2011. Imaging the impact of prenatal alcohol exposure on the structure of the developing human brain. Neuropsychol. Rev. 21 (2), 102–118. http://dx.doi.org/10.1007/s11065-011-9163-021369875.

Lehtelä, L., Salmelin, R., Hari, R., 1997. Evidence for reactive magnetic 10-Hz rhythm in the human auditory cortex. Neurosci. Lett. 222 (2), 111–114. http://dx.doi.org/10.1016/S0304-3940(97)13361-49111741.

Leigland, L.A., Ford, M.M., Lerch, J.P., Kroenke, C.D., 2013. The influence of fetal ethanol exposure on subsequent development of the cerebral cortex as revealed by magnetic resonance imaging. Alcohol. Clin. Exp. Res. http://dx.doi.org/10.1111/acer.1205123442156.

Malisza, K.L., Buss, J.L., Bolster, R.B., de Gervai, P.D., Woods-Frohlich, L., Summers, R., Clancy, C.A., Chudley, A.E., Longstaffe, S., 2012. Comparison of spatial working memory in children with prenatal alcohol exposure and those diagnosed with ADHD; a functional magnetic resonance imaging study. J. Neurodev. Disord. 4 (1), 12. http://dx.doi.org/10.1186/1866-1955-4-1222958510.

Mattson, S.N., Crocker, N., Nguyen, T.T., 2011. Fetal alcohol spectrum disorders: neuropsychological and behavioral features. Neuropsychol. Rev. 21 (2), 81–101. http://dx.doi.org/10.1007/s11065-011-9167-921503685.

Mattson, S.N., Riley, E.P., Gramling, L., Delis, D.C., Jones, K.L., 1998. Neuropsychological comparison of alcohol-exposed children with or without physical features of fetal alcohol syndrome. Neuropsychol. 12 (1), 146–153. http://dx.doi.org/10.1037/0894-4105.12.1.1469460742.

May, P.A., Gossage, J.P., 2001. Estimating the prevalence of fetal alcohol syndrome: a summary. Alcohol Res. Health 25 (3), 159–16711810953.

May, P.A., Gossage, J.P., Kalberg, W.O., Robinson, L.K., Buckley, D., Manning, M., Hoyme, H.E., 2009. Prevalence and epidemiologic characteristics of FASD from various

research methods with an emphasis on recent in-school studies. Dev. Disabil. Res. Rev. 15 (3), 176–192. http://dx.doi.org/10.1002/ddrr.6819731384.

Mazaheri, A., Jensen, O., 2010. Rhythmic pulsing: linking ongoing brain activity with evoked responses. Front. Hum. Neurosci. 4, 177.

Norman, A.L., O'Brien, J.W., Spadoni, A.D., Tapert, S.F., Jones, K.L., Riley, E.P., Mattson, S.N., 2013. A functional magnetic resonance imaging study of spatial working memory in children with prenatal alcohol exposure: contribution of familial history of alcohol use disorders. Alcohol. Clin. Exp. Res. 37 (1), 132–140. http://dx.doi.org/10.1111/j.1530-0277.2012.01880.x23072431.

O'Brien, J.W., Norman, A.L., Fryer, S.L., Tapert, S.F., Paulus, M.P., Jones, K.L., Riley, E.P., Mattson, S.N., 2013. Effect of predictive cuing on response inhibition in children with heavy prenatal alcohol exposure. Alcohol. Clin. Exp. Res. 37 (4), 644–654. http://dx.doi.org/10.1111/acer.1201723094678.

Oldfield, R.C., 1971. The assessment and analysis of handedness: the Edinburgh inventory. Neuropsychologia 9 (1), 97–113. http://dx.doi.org/10.1016/0028-3932(71)90067-45146491.

Plakke, B., Romanski, L.M., 2014. Auditory connections and functions of prefrontal cortex. Front. Neurosci. 8, 199. http://dx.doi.org/10.3389/fnins.2014.0019925100931.

Polich, J., 2007. Updating P300: an integrative theory of P3a and P3b. Clin. Neurophysiol. 118 (10), 2128–2148. http://dx.doi.org/10.1016/j.clinph.2007.04.01917573239.

Riley, E.P., Infante, M.A., Warren, K.R., 2011. Fetal alcohol spectrum disorders: an overview. Neuropsychol. Rev. 21 (2), 73–80. http://dx.doi.org/10.1007/s11065-011-9166-x21499711.

Roussotte, F., Soderberg, L., Sowell, E., 2010. Structural, metabolic, and functional brain abnormalities as a result of prenatal exposure to drugs of abuse: evidence from neuroimaging. Neuropsychol. Rev. 20 (4), 376–397. http://dx.doi.org/10.1007/s11065-010-9150-x20978945.

Sadrian, B., Wilson, D.A., Saito, M., 2013. Long-lasting neural circuit dysfunction following developmental ethanol exposure. Brain Sci. 3 (2), 704–727. http://dx.doi.org/10.3390/brainsci302070424027632.

Sickmann, H.M., Patten, A.R., Morch, K., Sawchuk, S., Zhang, C., Parton, R., Szlavik, L., Christie, B.R., 2014. Prenatal ethanol exposure has sex-specific effects on hippocampal long-term potentiation. Hippocampus 24, 54–64. http://dx.doi.org/10.1002/hipo.2220323996604.

Soltani, M., Knight, R.T., 2000. Neural origins of the P300. Crit. Rev. Neurobiol. 14 (3–4), 199–224. http://dx.doi.org/10.1615/CritRevNeurobiol.v14.i3-4.2012645958.

Sowell, E.R., Mattson, S.N., Kan, E., Thompson, P.M., Riley, E.P., Toga, A.W., 2008. Abnormal cortical thickness and brain-behavior correlation patterns in individuals with heavy prenatal alcohol exposure. Cereb. Cortex 18 (1), 136–144. http://dx.doi.org/10.1093/cercor/bhm03917443018.

Sowell, E.R., Thompson, P.M., Mattson, S.N., Tessner, K.D., Jernigan, T.L., Riley, E.P., Toga, A.W., 2002. Regional brain shape abnormalities persist into adolescence after heavy prenatal alcohol exposure. Cereb. Cortex 12 (8), 856–865. http://dx.doi.org/10.1093/cercor/12.8.85612122034.

Spottiswoode, B.S., Meintjes, E.M., Anderson, A.W., Molteno, C.D., Stanton, M.E., Dodge, N.C., Gore, J.C., Peterson, B.S., Jacobson, J.L., Jacobson, S.W., 2011. Diffusion tensor imaging of the cerebellum and eyeblink conditioning in fetal alcohol spectrum disorder. Alcohol. Clin. Exp. Res. 35 (12), 2174–2183. http://dx.doi.org/10.1111/j.1530-0277.2011.01566.x21790667.

Steinmann, T.P., Andrew, C.M., Thomsen, C.E., Kjær, T.W., Meintjes, E.M., Molteno, C.D., Jacobson, J.B., Jacobson, S.W., Sorensen, H.B., 2011. An auditory go/no-go study of event-related potentials in children with fetal alcohol spectrum disorders. Conf.

Proc. IEEE Eng. Med. Biol. Soc. 2011, 789–792. http://dx.doi.org/10.1109/IEMBS.2011.609018122254429.

Stephen, J.M., Kodituwakku, P.W., Kodituwakku, E.L., Romero, L., Peters, A.M., Sharadamma, N.M., Caprihan, A., Coffman, B.A., 2012. Delays in auditory processing identified in preschool children with FASD. Alcohol. Clin. Exp. Res. 36 (10), 1720–1727. http://dx.doi.org/10.1111/j.1530-0277.2012.01769.x22458372.

Stratton, K., Howe, C., Battaglia, F.P., Institute of Medicine, 1996. Fetal Alcohol Syndrome: Diagnosis, Epidemiology, Prevention, and Treatment. National Academies Press, Washington.

Swick, D., Chatham, C.H., 2014. Ten years of inhibition revisited. Front. Hum. Neurosci. 8 (329), 329. http://dx.doi.org/10.3389/fnhum.2014.0032924904369.

Tadel F., Baillet S., Mosher J.C, Pantazis D., Leahy R.M., Brainstorm: A user-friendly application for MEG/EEG analysis. Comput. Intell. Neurosci., 2011 (2011) 879716, ID 879716. [doi:10.1155/2011/879716] [Pubmed: 21584256]

Taulu, S., Simola, J., 2006. Spatiotemporal signal space separation method for rejecting nearby interference in MEG measurements. Phys. Med. Biol. 51 (7), 1759–1768. http://dx.doi.org/10.1088/0031-9155/51/7/00816552102.

Tesche, C.D., Uusitalo, M.A., Ilmoniemi, R.J., Huotilainen, M., Kajola, M., Salonen, O., 1995. Signal-space projections of MEG data characterize both distributed and well-localized neuronal sources. Electroencephalogr. Clin. Neurophysiol. 95 (3), 189–200. http://dx.doi.org/10.1016/0013-4694(95)00064-67555909.

Tiihonen, J., Hari, R., Kajola, M., Karhu, J., Ahlfors, S., Tissari, S., 1991. Magnetoencephalographic 10-Hz rhythm from the human auditory cortex. Neurosci. Lett. 129 (2), 303–305. http://dx.doi.org/10.1016/0304-3940(91)90486-D1745412.

Treit, S., Lebel, C., Baugh, L., Rasmussen, C., Andrew, G., Beaulieu, C., 2013. Longitudinal MRI reveals altered trajectory of brain development during childhood and adolescence in fetal alcohol spectrum disorders. J. Neurosci. 33 (24), 10098–10109. http://dx.doi.org/10.1523/JNEUROSCI.5004-12.201323761905.

Weisz, N., Hartmann, T., Müller, N., Lorenz, I., Obleser, J., 2011. Alpha rhythms in audition: cognitive and clinical perspectives. Front. Psychol. 2, 73. http://dx.doi.org/10.3389/fpsyg.2011.0007321687444.

Wilson, D.A., Peterson, J., Basavaraj, B.S., Saito, M., 2011. Local and regional network function in behaviorally relevant cortical circuits of adult mice following postnatal alcohol exposure. Alcohol. Clin. Exp. Res. 35 (11), 1974–1984. http://dx.doi.org/10.1111/j.1530-0277.2011.01549.x21649667.

Wozniak, J.R., Mueller, B.A., Muetzel, R.L., Bell, C.J., Hoecker, H.L., Nelson, M.L., Chang, P.N., Lim, K.O., 2011b. Inter-hemispheric functional connectivity disruption in children with prenatal alcohol exposure. Alcohol. Clin. Exp. Res. 35 (5), 849–861. http://dx.doi.org/10.1111/j.1530-0277.2010.01415.x21303384.

Wozniak, J.R., Muetzel, R.L., 2011a. What does diffusion tensor imaging reveal about the brain and cognition in fetal alcohol spectrum disorders? Neuropsychol. Rev. 21 (2), 133–147. http://dx.doi.org/10.1007/s11065-011-9162-121347880.

Wunderlich, J.L., Cone-Wesson, B.K., Shepherd, R., 2006. Maturation of the cortical auditory evoked potential in infants and young children. Hear. Res. 212 (1–2), 185–202. http://dx.doi.org/10.1016/j.heares.2005.11.01016459037.

Yang, Y., Roussotte, F., Kan, E., Sulik, K.K., Mattson, S.N., Riley, E.P., Jones, K.L., Adnams, C.M., May, P.A., O'Connor, M.J., Narr, K.L., Sowell, E.R., 2012. Abnormal cortical thickness alterations in fetal alcohol spectrum disorders and their relationships with facial dysmorphology. Cereb. Cortex 22 (5), 1170–1179. http://dx.doi.org/10.1093/cercor/bhr19321799209.